MODELING AND CONTROL OF 3-Φ GRID CONNECTED INVERTER SYSTEM FOR DISTRIBUTED POWER GENERATION SYSTEM

Tusar Kumar Dash

Department of Electrical Engineering

National Institute of Technology, Rourkela

Rourkela-769008, Odisha, INDIA

May 2013

MODELING AND CONTROL OF 3-Φ GRID CONNECTED INVERTER SYSTEM FOR DISTRIBUTED POWER GENERATION SYSTEM

A Thesis Submitted in Partial Fulfilment of the

Requirements for the Degree of

Master of Technology

in

Electrical Engineering

by

Tusar Kumar Dash

(Roll no-211EE2129)

Under the Guidance of

Prof. B. Chitti Babu

Department of Electrical Engineering

National Institute of Technology, Rourkela

Rourkela-769008, Odisha, INDIA

May 2013

Dedicated to my beloved Parents and my Brother

ACKNOWLEDGEMENTS

I would like to express my sincere gratitude to my supervisor **Prof. B. Chitti Babu** for his guidance, encouragement, and support throughout the course of this work. It was an invaluable learning experience for me to be one of his students. From him I have gained not only extensive knowledge, but also a sincere research attitude.

I express my gratitude to **Prof. A.K Panda,** Head of the Department, Electrical Engineering for his invaluable suggestions and constant encouragement all through the research work.

My thanks are extended to my friends Tulika, Avinash, Debasis, Gouri, Sachin in "Power Control 'N' Drives," who built an academic and friendly research environment that made my study at NIT, Rourkela most memorable and fruitful.

I would also like to acknowledge the entire teaching and non-teaching staff of Electrical Department for establishing a working environment and for constructive discussions.

Finally, I am always indebted to all my family members Bhaina, Bhauja, Guduli especially my parents, for their endless love and blessings.

Tusar Kumar Dash
Roll - no.:- 211EE2129

DEPARTMENT OF ELECTRICAL ENGINEERING

NATIONAL INSTITUTE OF TECHNOLOGY ROURKELA

ODISHA, INDIA

CERTIFICATE

This is to certify that the Thesis Report entitled "**MODELING AND CONTROL OF 3-Φ GRID CONNECTED INVERTER SYSTEM FOR DISTRIBUTED POWER GENERATION SYSTEM",** submitted by Mr. TUSAR KUMAR DASH bearing roll no. 211EE2129 in partial fulfillment of the requirements for the award of Master of Technology in Electrical Engineering with specialization in "Power Control and Drives" during session 2011-2013 at National Institute of Technology, Rourkela is an authentic work carried out by him under our supervision and guidance.

To the best of our knowledge, the matter embodied in the thesis has not been submitted to any other university/institute for the award of any Degree or Diploma.

Date:

Place: Rourkela

Prof. B. Chitti Babu

Department of Electrical Engineering

National Institute of Technology

Rourkela-769008

Email: bcbabunitrkl@gmail.com

CONTENTS

Abstract i

List of figures ii

List of tables iv

Acronyms v

CHAPTER 1

1.1 Introduction 1

1.2 Research motivation 2

1.3 Literature review 3

1.4 Thesis objectives 5

1.5 Thesis organisation 5

CHAPTER 2

2.1 Small signal model of 1-Φ inverter 7

CHAPTER 3

3.1 Control strategy for 1-Φ inverter 11

3.1.A Proportional Resonant controller 11

3.1.1.A Current control scheme 15

3.1.1.B Voltage control scheme 17

3.1.1.B.1 PI voltage controller 18

3.1.1.B.2 Resonant voltage controller 19

CHAPTER 4

4.1 Modelling of 3-Φ inverter 22

4.1.1 Power stage model 22

4.1.2 Small signal model 24

CHAPTER 5

5.1 Transfer function and Bode plots 27

5.1.1 Control to d-axis current transfer function 27

5.1.2 Control to d-axis voltage transfer function 27

5.2 Control strategy for 3-Φ inverter 29

CHAPTER 6

6.1 Results and discussion

6.1.1 1-Φ inverter

6.1.1.A With PI voltage controller 31

6.1.1.B With Resonant voltage controller 33

6.1.1.C Comparison of THD% 35

6.1.2 3-Φ inverter 36

CHAPTER 7

7.1 Conclusion and future work 37

References 38

Appendix A 40

Publications 41

ABSTRACT

At present scenario, renewable energy sources become an alternative source of energy for future energy demand and to mitigate environment pollution problems. Grid connected renewable energy source like wind energy system uses power electronics converters as an interfacing device between wind energy system and utility grid. These converters are commonly based on a voltage source inverter (VSI) connected to the supply network, operated to achieve objectives such as power flow regulation with unity power factor operation. However, intermittent nature of wind energy must be controlled to meet the grid requirements. The grid requirements include independent control of active & reactive power, improved power quality, grid synchronization and Good transient response during fault conditions etc. Usually voltage oriented control (VOC) of grid side converter in the synchronous reference frame was universally adapted for independent control of active and reactive power of the grid. However, the dynamic response during abnormal condition of grid is sluggish and poor power quality. In order to design controller for robust performance and to know the control characteristics, VSI needs to be accurately modelled. This project has taken an attempt to derive the small signal model of a single phase inverter in isolated mode and its performance with different controllers. Further, the work is extended to modelling of three phase grid connected VSI and its relevant transfer functions have been deduced from the model so as to analyse the system performance for designing a controller through well-known bode plots. The studied system is modelled and simulated in the MATLAB-Simulink environment.

LIST OF FIGURES

Fig. No.	Fig. Description	Page No.
Fig. 1.1	General structure of Distributed Generation system	1
Fig. 2.1	Schematic diagram of 1-Φ inverter to be modelled	7
Fig. 2.2	Equivalent circuit when switches S_1 and S_2 are ON	8
Fig. 2.3	Equivalent circuit when switches S_3 and S_4 are ON	8
Fig. 2.4	Small signal model of 1-Φ inverter	10
Fig. 3.1	Single phase equivalent presentation of PR controller	12
Fig. 3.2	Bode plots of ideal PR controller	14
Fig. 3.3	Bode plots of non-ideal PR controller	15
Fig. 3.4	Control loop for ACC strategy	16
Fig. 3.5	Bode plot of $Gi_Ld(s)$	16
Fig. 3.6	Bode plot of current loop	17
Fig. 3.7	Bode plot of $G_{v_0-v_c}$	18
Fig. 3.8	ACC with PI controller	18
Fig. 3.9	Bode plot of voltage loop with PI controller	19
Fig. 3.10	ACC with P+Resonant controller	20
Fig. 3.11	Bode plot of voltage loop with P+ Resonant controller	21
Fig. 4.1	Schematic diagram of three phase grid connected VSI with LC filter	22
Fig. 4.2	Power stage model of three phase grid connected VSI	24
Fig. 4.3	Small signal model of three phase grid connected VSI	26
Fig. 5.1	Control to grid voltage transfer function bode plot	27
Fig. 5.2	Control to grid voltage transfer function bode plot	28
Fig. 5.3	Control structure of 3-Φ grid connected VSI	29
Fig. 6.1	Output voltage V_0 of 1-Φ inverter (linear load) (PI voltage controller)	31
Fig. 6.2	Output current i_0 of 1-Φ inverter (linear load) (PI voltage controller)	31
Fig. 6.3	THD of output voltage for linear load (PI voltage controller)	32
Fig. 6.4	Output voltage V_0 of 1-Φ inverter (non-linear load) (PI voltage controller)	32
Fig. 6.5	Output current i_0 of 1-Φ inverter (non-linear load) (PI voltage controller)	32
Fig. 6.6	THD of output voltage for non-linear load (PI voltage controller)	33
Fig. 6.7	Output voltage V_0 of 1-Φ inverter (linear load) (P+ Resonant voltage	33

controller)
Fig. 6.8 Output voltage i_0 of 1-Φ inverter (linear load) (P+ Resonant voltage controller) 33
Fig. 6.9 THD of output voltage for linear load (PI voltage controller) 34
Fig. 6.10 Output voltage V_0 of 1-Φ inverter (non-linear load) (P+ Resonant voltage controller) 34
Fig. 6.11 Output voltage i_0 of 1-Φ inverter (linear load) (P+ Resonant voltage controller) 34
Fig. 6.12 THD of output voltage for non-linear load(P+ Resonant voltage controller) 35
Fig. 6.13 Step response of dc link voltage controller 35
Fig. 6.14 Step response of current controller 36
Fig. A1 Transformation of three phases to stationary α-β reference frame 40
Fig. A2 Transformation of three phases to stationary α-β reference frame 41

LIST OF TABLES

No.	Table content	Page No.
3.1	Resonant Controller Parameters	20
3.2	System Parameters (1-Φ)	21
5.1	System Parameters (3-Φ)	28

ACRONYMS

V_{dc}	Dc supply voltage
S_1,S_2,S_3,S_4,S_5,S_6	Switches
L	Filter inductance
C	Filter capacitance
R_c	Damping resistance
R	Load resistance
i_L	Inductor current
i_c	Capacitor current
I_0	Load current
V_c	Voltage across capacitor
V_0	Output voltage
T_s	Switching period
d	Duty cycle
I_s	Source current
$\widehat{v_{dc}}$	Perturbation in dc voltage
$\widehat{v_0}$	Perturbation in output voltage
$\hat{d}$	Perturbation in duty cycle
$\widehat{i_L}$	Perturbation in inductor current
$\widehat{v_c}$	Perturbation in capacitor voltage
I_L	Inductor current at defined operating point
D	Duty cycle at defined operating point
F_m	Gain of pulse width modulator
RD	Digital delay
R_i	Gain of current sensor
$Gi_Ld(s)$	Duty cycle to output current transfer function
Z	Load impedance
K_p	Proportional gain

K_1	Gain of resonant controller of ACC
B_1	Bandwidth of resonant controller of ACC
ω_1	Resonant angular frequency
$G_{v0\text{-}vc}(s)$	Control to output voltage transfer function
β	Gain of voltage sensor
$T_v(s)$	Voltage control loop transfer function
h	Harmonic order
K_h	Gain of h^{th} harmonic
B_h	Bandwidth of h^{th} harmonic
i	Input dc current
V_{Ai}	Inverter output voltage for phase-A
V_{Bi}	Inverter output voltage for phase-B
V_{Ci}	Inverter output voltage for phase-C
i_A	Output current for phase-A
i_B	Output current for phase-B
i_C	Output current for phase-C
V_{Ag}	Grid voltage phase-A
V_{Bg}	Grid voltage phase-B
V_{Cg}	Grid voltage phase-C
V_{di}	D-axis inverter output voltage
V_{qi}	Q-axis inverter output voltage
V_{dg}	D-axis grid voltage
V_{qg}	Q-axis grid voltage
i_d	D-axis current
i_q	Q-axis current
d_d	D-axis duty cycle
d_q	Q-axis duty cycle
$\widehat{\imath_d}$	D-axis current perturbation
$\widehat{\imath_q}$	Q-axis current perturbation
$\widehat{v_{dg}}$	D-axis grid voltage
$\widehat{v_{qg}}$	Q-axis grid voltage
$\widehat{d_d}$	D-axis duty cycle perturbation
$\widehat{d_q}$	Q-axis duty cycle perturbation

$\hat{\imath}$	Dc input current perturbation
ω_0	Resonant frequency
K_i	Gain of integral controller
ω_c	Cut-off frequency

CHAPTER 1

1.1 Introduction

Due to exponential growth of future energy demand and depletion of fossil fuels, renewable energy sources are playing a pivotal role in the today power scenario. Renewable energy sources include wind power, PV system, bio mass, wave energy and small hydro etc. Among all renewable energy sources, wind energy system is most promising source of energy due to economic viability [1].

Distributed generation (DG) based on renewable energy sources are basically small scale power generation units (typically ranges from 20 kW to 20 MW) and they are located at the end user without long distance transmission line. As a result, it reduces the transportation cost of generation and consumption points are close to each other. It is feasible to implement interfaces having ability to operate in grid connected as well as in isolated mode without grid connection which is called micro grids [2]. The basic structure of a Distributed Power Generation System (DPGS) is illustrated in Fig.1.1.

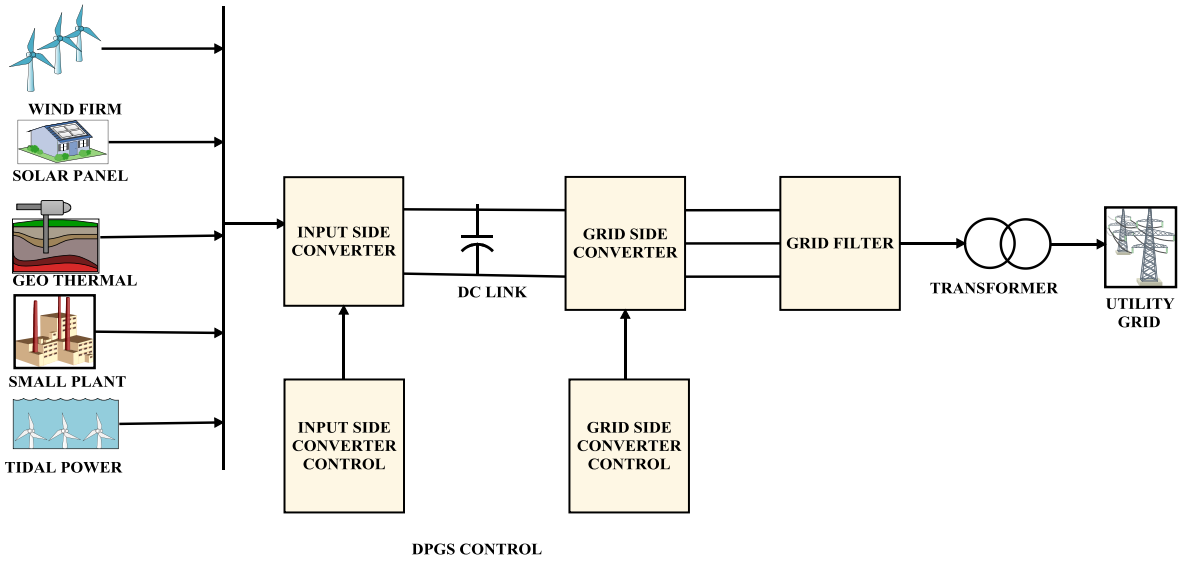

Fig.1.1 General structure of Distributed Generation system

The input to the DPGS can be sources like wind firm, solar panel, geothermal, tidal turbine, and small plants as portrayed in the above figure. Then back to back converters are connected so as to control the output voltage and frequency due to inconsistency of the input sources to meet the load or grid requirements Moreover, it provides bidirectional power flow between

the sources and grid. The role of input side converter is to extract the maximum power from the renewable source and to provide the power to grid side converter. The role of grid side converter is to control the power flow to the grid and to maintain the output voltage and frequency at the desired level. The system is synchronised with the grid through a filter known as grid filters. These filters require high switching frequencies to acceptably attenuate switching harmonics particularly in weak grid where the grid voltage is sensitive to load variations. In most cases control design for the three phase PWM inverter involves two steps and these are choice of modulation strategy which corresponds to open loop control and design of dynamic close loop control. However, reactive power control is one of the key issues to deal with in DPGS. From the investigation of the blackout occurred in U.S. and Canada in 2003 it was found that the cascaded outages of several transmission lines and generating units could have been avoided if controllable reactive power was available [3].

This project has taken an attempt to derive the small signal model of a single phase inverter in isolated mode and its performance with different controllers. Further, the work is extended to modelling of three phase grid connected VSI and its relevant transfer functions have been deduced from the model so as to analyse the system performance for designing a controller through well-known bode plots. The studied system is modelled and simulated in the MATLAB-Simulink environment.

1.2 Research Motivation

In recent years availability of power in India has both increased and improved but demand has consistently outstripped supply and substantial energy and peak shortages prevailed in 2009-10. Due to economic viability wind energy has become promising source of renewable energy. Now India has become fifth in installed capacity of wind power plant. As of 31st march the installed capacity of wind power in India was 17967MW [4]. But, as the wind is season and region based, it was not so reliable as long as Power Electronics had not been advanced much. Now-a-days the interface of Power Electronics has made wind energy system one of the reliable sources. Still there are some problems regarding stability and synchronization with utility grid, which has been improved by employing new control

algorithms to switch the PWM based voltage source inverter used in it. An attempt is initiated to improve the control of Grid side inverter in this project.

1.3 Literature Review

Grid connected inverter system employes different control algorithm in order to improve the over all system perfomance and the relevent control strategies are extensively studied in the available literature[1]-[18]. Average current control (ACC) has been widely used for controlling DC/DC as well as single-phase power factor correction (PFC) converters. Compared to peak current control ACC has following advantages[5].

- Error is minimized as a high gain current error amplifier is used.
- Large noise margin.
- No need of external compensation ramp.
- Easy current limit implementation.
- Good tracking performance of Average current mode control.

In order to design an average current control for an inverter, small signal modelling needs to be done which is based on average switched modelling [5]. In this technique manipulations are performed on the circuit rather than on its equations. The converter switches are replaced with voltage and current sources to obtain a time invariant circuit. Then the converter wave forms are averaged over one switching period to remove the undesired switching harmonics. Any non-linear elements present in the averaged circuit model can then be perturbed and linearized to represent small signal model [6]. In order to implement average current controller small signal modelling of inverter is required. This can be achieved by circuit averaging and as well as state space averaging. In [7] a state space averaging method is employed so as to get a small signal model. In [8] an average current mode controller is used to get equal current distribution in case of a resonant DC to DC converter. In average model of three phases inverter is proposed so as to reduce the current distributions in multi module Resonant dc to dc converter. However, in case of three phase grid connected inverter voltages and currents are usually transferred to rotating d-q reference frame for making design of controller easier because the current space vector in the rotating d-q reference frame is fixed, the PI controllers operate on dc, rather than sinusoidal signals. A new and simpler control

technique is being employed in a grid connected inverter without applying the d-q transformation as reported in [9] which achieves zero steady state error in the stationary reference frame. A new predictive control algorithm for grid-connected current-controlled inverters is being employed in [10] which combine a two-sample deadbeat control law with a Luenberger observer to estimate the future value of the grid currents. The resulting control offers robustness against the computational delay inherent in the digital implementation and considerably enhances the gain and phase margins of the previous predictive controls while maintaining the high-speed response of the deadbeat controllers. A novel control for voltage-source inverters with the capability to flexibly operate in grid-connected and islanded modes was studied designed in [11] which are based on the droop method, which uses some estimated grid parameters such as the voltage and frequency and the magnitude and angle of the grid impedance. Hence, the inverter is able to inject independently controlled active and reactive power to the grid. The controller provides a proper dynamics decoupled from the grid-impedance magnitude and phase. The system is also able to control active and reactive power flows independently for a large range of impedance grid values. For controlling reactive power a new control strategy direct current d-q vector control has been proposed in [12] to overcome the shortage of the conventional vector control technique. Direct control technique differs from standard vector control technique in the generation of control variable. In the former case current is the tuned control variable and in latter case is the voltage. However, in almost all the cases of the control techniques of three phase grid connected inverter transformation to rotating co-ordinates have been employed but in [13] direct power control is followed which utilises a non-linear sliding mode control in order to reduce the instantaneous power error to zero and this does not necessitate transformation to rotating co-ordinates. To design a controller for inverter transfer functions are to be derived and in order to accomplish that it is to be modelled. In [14] a single phase inverter in island mode is modelled as small signal model and then transfer functions are derived for designing an Average current controller (ACC) for it. A switching flow-graph (SFG) modelling technique [16] is used to build the large-signal model of a cascaded multilevel inverter. With the concept of virtual switch and virtual switching function proposed in SFG modelling technique, the large-signal SFG model of a cascaded multilevel inverter can be derived easily and without complex mathematic works. A novel control method, named weighted average cur-rent control (WACC), is proposed for damping control of a three-phase grid inverter with an LC filter [17]. In this method, the sum of partial inverter current and partial grid current is used as the feedback of the current control loop. By using WACC, three-phase current control

of the grid inverter can be well decoupled under synchronous rotating frame. Furthermore, the system transfer function is reduced from the third-order system to the first-order system. Consequently, the control loop gain and bandwidth can be increased, which improve the rejection capability to the back-ground grid voltage harmonics.

1.4 Thesis Objectives

The ultimate aim of this study is to meet the following objectives:

- To derive a small signal modelling of 1-Φ inverter and its transfer functions for designing controller.
- To extend small signal modelling to 3-Φ grid connected inverter.
- To derive transfer functions of modelled grid connected inverter and observe the effect of resonance from the bode plots.
- To design a controller for three phase grid connected inverter based on derived small signal model.

1.5 Thesis Organization

The organisation of thesis is given as follows

CHAPTER 1 which describes the research motivation and related work done of proposed study. Also it advises the objectives of the proposed study.

CHAPTER 2 presents the modelling of 1-Φ inverter with LC filter and R-load which is based on the principle of perturb and observe.

CHAPTER 3 presents the control loop design of the current and voltage control loop and the analysis has been done in order to observe the stability of the system by plotting Bode plots. Transfer functions of control loops are being deduced from the derived small signal model. An average current control is designed for the 1-Φ inverter and THD% of output voltages are compared by using PI voltage control and P+Resonant control technique.

CHAPTER 4 presents the modelling of 3-Φ grid connected inverter which involves two stages of modelling. One is power stage modelling and from the power stage model small signal model is derived which is based on same principle perturb and observe.

CHAPTER 5 presents the control loop design for both voltage and current and also the transfer functions are derived for stability study. The effect of resonance was observed from the bode plot of control to grid voltage transfer function. A control strategy is developed with step responses of the controller for effectiveness of the study.

CHAPTER 6 presents the simulation results which are being carried out in MATLAB/Simulink environment.

CHAPTER 7 presents the conclusion of work done and scope of the future work followed by references.

CHAPTER 2

2.1 Small Signal Model of 1-Φ Inverter

The main objective of studying small signal model is to predict low frequency component present in the output voltage [6]. The magnitude and phase of this component depend not only on the duty cycle variation but also frequency response of the converter. It is obtained by giving a deliberate perturbation around the operating point and then linearizing it at that point. The 1-Φ full bridge VSI system is illustrated in Fig.2.1.

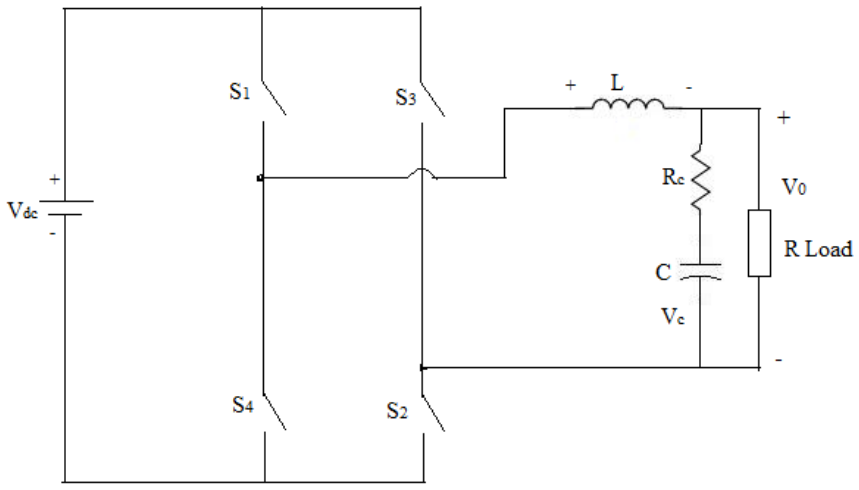

Fig.2.1 Schematic diagram of 1-Φ inverter to be modelled

The inverter in the above figure is being modelled and analysed with LC filter on the load side which considers R as load.

Let's consider

V_{dc} is Supply dc voltage

S_1 ,S_2 ,S_3 ,S_4 are switches

L is filter inductance

R_c is damping resistor

C is filter capacitor

R is load resistance

The main purpose of using the damping resistor is to damp out the oscillations occurring due to the use of LC filter resonance.

Case 1

When switches S_1 and S_2 are ON, then circuit is shown in Fig.2.2.

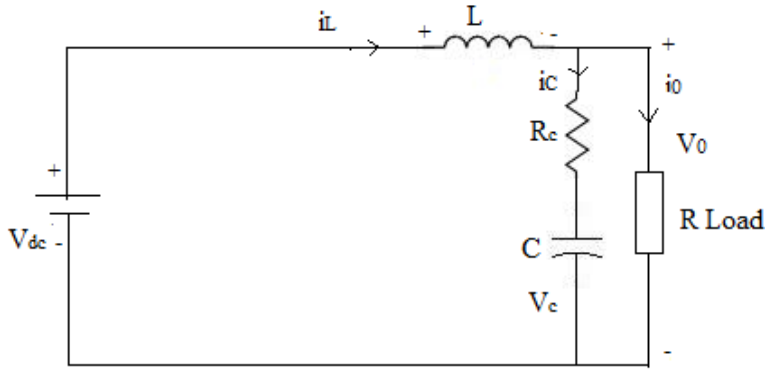

Fig 2.2 Equivalent circuit when switches S_1 and S_2 are ON

Applying KVL in Fig 2.2

$$L\frac{di_L}{dt} = V_{dc} - V_0 \tag{2.1}$$

And

$$i_C = i_L - i_0$$

$$C\frac{dV_c}{dt} = i_L - \frac{V_0}{R} \tag{2.2}$$

Case 2

When switches S_3&S_4 are ON, the resultant circuit will be as shown in Fig.2.3.

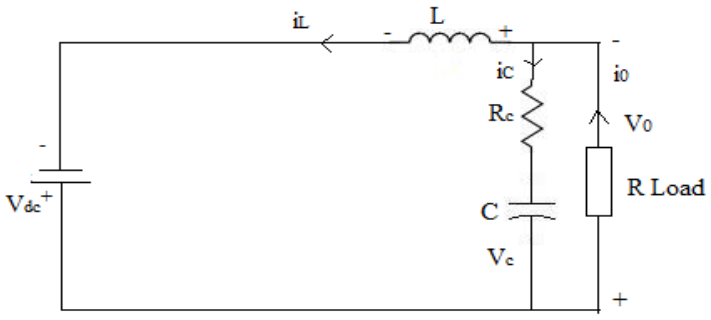

Fig.2.3 Equivalent circuit when switches S_3 and S_4 are ON

By applying KVL in the above circuit

$$L\frac{di_L}{dt} = V_0 - V_{dc} \quad (2.3)$$

And

$$i_C = -i_L - i_0$$

$$C\frac{dV_c}{dt} == -i_L - \frac{V_0}{R} \quad (2.4)$$

Let's consider average value of the inductor current and capacitor voltage over a switching period T_s.

$$\Rightarrow L\frac{d<i_L>_{T_s}}{dt} = d.< V_{dc} - V_0 >_{T_s} + d'.< V_0 - V_{dc} >_{T_s} \quad (2.5)$$

Where d= duty cycle $and\ d' = 1 - d$

$$\text{And } C\frac{d<V_c>_{T_s}}{dt} = d.< i_L - \frac{V_0}{R} >_{T_s} + d' < -i_L - \frac{V_0}{R} >_{T_s} \quad (2.6)$$

Let's define an operating point as follows

Duty cycle = D

Input voltage =V_{dc}

Output voltage = V_0

Capacitor voltage= V_c

Inductor current= I_L

Source current = I_s

In order to design a small signal model we will have to consider a small perturbation along with its steady state values.

$$< V_{dc} >_{T_s} = V_{dc} + \widehat{v_{dc}}$$

$$< V_0 >_{T_s} = V_0 + \widehat{v_0}$$

$$< D >_{T_s} = D + \hat{d}$$

$< I_L >_{T_s} = I_L + \hat{\imath_L}$

$< V_C >_{T_s} = V_C + \widehat{v_C}$

Putting above values in equation (2.5) and (2.6)

$$L\frac{d(I_L+\hat{\imath_L})}{dt} = \left(D+\hat{d}\right) * \{V_{dc} + \widehat{v_{dc}} - V_0 - \widehat{v_0}\} + \left(1-D-\hat{d}\right) * \{-V_{dc} - \widehat{v_{dc}} + V_0 + \widehat{v_0}\} \quad (2.7)$$

On simplification the equation (2.7) gives rise to multiplication of steady state value terms along with linear and non-linear terms. Multiplication of perturbation terms can be neglected as its results are very small. So resulting expression would be

$$L\frac{d\hat{\imath_L}}{dt} = (D-D')\widehat{v_{dc}} - (D-D')\widehat{v_0} + 2V_0\hat{d} = (2D\text{-}1)\widehat{v_{dc}} - (2D-1)\widehat{v_0} + 2V_{dc}\hat{d} \quad (2.8)$$

Similarly

$$C\frac{d\widehat{v_C}}{dt} = (2D-1)\hat{\imath_L} - \frac{\widehat{v_0}}{R} + 2I_L\hat{d} \quad (2.9)$$

From the equations (2.8) & (2.9) small signal model of the inverter is derived and is depicted in Fig.2.4.

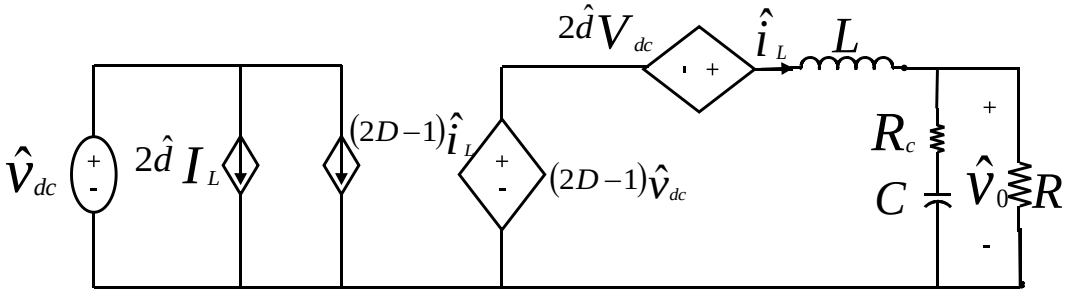

Fig 2.4 Small signal model of 1-Φ inverter

From Fig 2.4 it can be observed that a small signal ac current $\hat{\imath_L}$ is drawn by the inverter out of the input voltage source $\widehat{v_{dc}}$. As the concerned VSI of bridge type configuration the duty cycle is (2D-1). The term $(2D-1)\hat{\imath_L}$ is dependent on the inductor current variation $\hat{\imath_L}$ and is represented by a dependent source. The term $2\hat{d}I_L$ is driven by the control variations and is modelled by an independent source. This is an equivalent circuit that models the low frequency small signal variations in the inverter waveforms and it can be solved to using conventional linear circuit analysis techniques to find the inverter transfer functions.

CHAPTER 3

3.1 Control Strategy for 1-Φ Inverter

A control scheme is to be employed to make the output voltage of the inverter to be sinusoidal and hence to reduce THD in it. In this project an ACC [7] has been implemented to control the inductor current and PI controller or Resonant controller for controlling output voltage.

3.1.A Proportional Resonant (PR) controller

In order to alleviate the short comings associated with conventional PI controller a novel controller proportional resonant controller [PR] is introduced recently. The shortcomings of conventional PI controller are considerable steady-state errors in single-phase systems and the need for synchronous d–q transformation [17] in three-phase systems. PR control theory used in filters which is used for generating the harmonic command reference in an active power filter, especially for single-phase systems, where d–q transformation theory is not directly applicable. Another advantage associated with the PR controllers and filters is the possibility of implementing selective harmonic compensation without requiring excessive computational resources. Besides the above advantages the superior performance of PR controller in tracking sinusoidal waveforms is the one which made it quite familiar among researchers. However, according to Internal Model Control Principle [19] the value of resonant frequency is necessitated inside the control model. For the design of PR controller the nominal value of grid frequency and its multiple values are used but when the grid frequency experiences fluctuations, the performance of PR controller deteriorates.

PR controllers are equivalent to conventional PI controller implemented in two synchronous rotating frames (positive sequence and negative sequence) and hence able to track sinusoidal references with variable frequency of both positive and negative sequences with zero steady state error. The transfer function of PR controller can be derived by using internal control model with modified state transformation or frequency domain approach. [21]

As d-q transformation can't be applied to single phase system directly, a new method is adopted by multiplying sine and cosine functions resulting from phase locked loop with the feedback error signal e(t) as shown in Fig. 3.1.

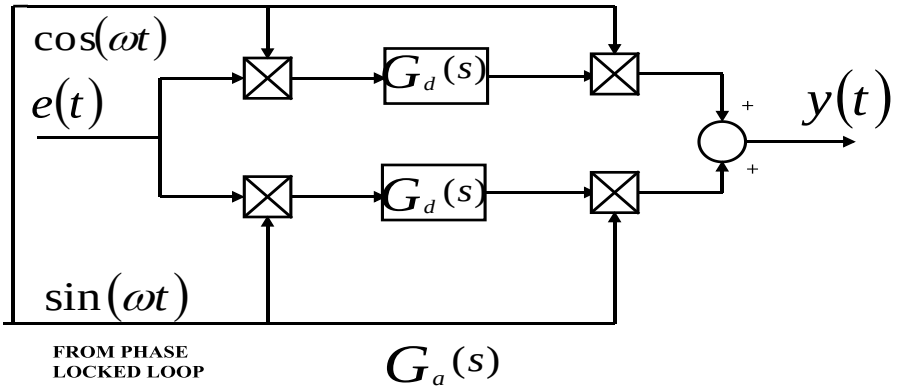

Fig. 3.1 Single phase equivalent presentation of PR controller

This achieves the same effect of transforming the component at chosen frequency to dc quantity leaving others to ac quantities.

Let's assume the feedback error signal contains fundamental component along with fifth harmonic component which is expressed by equation (3.1)

$$e(t) = E_1 \cos(\omega t + \Phi_1) + E_5 \cos(5\omega t + \Phi_5) \tag{3.1}$$

Where ω, Φ_1, Φ_5 are the fundamental angular frequency, fundamental and fifth harmonic phase shifts respectively.

Multiplying equation (3.1) by sin(ωt) and cos(ωt) respectively equations (3.2) and (3.3) are derived

$$e(t).\cos(\omega t) = \frac{E_1}{2}\{\cos(\Phi_1) + \cos(2\omega t + \Phi_1)\} + \frac{E_5}{2}\{\cos(6\omega t + \Phi_5) + \cos(4\omega t + \Phi_5)\} \tag{3.2}$$

$$e(t).\sin(\omega t) = \frac{E_1}{2}\{\sin(-\Phi_1) + \sin(2\omega t + \Phi_1)\} + \frac{E_5}{2}\{\sin(6\omega t + \Phi_5) + \sin(-4\omega t - \Phi_5)\} \tag{3.3}$$

From equations (3.2) and (3.3) it is observed that the fundamental component of feedback error signal is a constant as it is a function of phase shift Φ_1 only. The only complication with this equivalent single-phase conversion is that the chosen frequency component not only appears as a dc quantity in the synchronous frame, it also contributes to harmonic terms at a frequency of 2ω, unlike three phase synchronous d–q conversion. However, passing equations (3.2) & (3.3) through integral blocks would still force the fundamental error amplitude E_1 to zero, caused by the infinite gain of the integral blocks.

Instead of transforming the feedback error to the equivalent synchronous frame for processing, an alternative approach of transforming the controller $G_d(s)$ from the synchronous to the stationary frame is also possible. The ac quantity which includes the dc controller $G_d(s)$ can be expressed by equation (3.4) after taking positive and negative sequence components into consideration.

$$G_a(s) = G_d(s)(s + j\omega) + G_d(s)(s - j\omega) \tag{3.4}$$

Where $G_a(s)$ is the equivalent stationary frame transfer function.

For ideal integrator $G_d(s) = \frac{K_i}{s}$ and by substituting in equation (3.4) $G_a(s)$ can be derived as follows

$$G_a(s) = \frac{Y(s)}{E(s)} = \frac{2K_i s}{s^2+\omega^2} \tag{3.5}$$

For non-ideal integrator $G_d(s) = \frac{K_i}{1+\frac{s}{\omega_c}}$ and by substituting in equation (3.4) $G_a(s)$ can be derived as follows

$$G_a(s) = \frac{Y(s)}{E(s)} = \frac{2K_i\omega_c s}{s^2+2\omega_c s+\omega^2} \tag{3.6}$$

Where K_i and ω_c are the integral controller gain and cut-off frequency respectively.

Equation (3.5) when grouped with a proportional term K_p gives the ideal PR controller with an infinite gain at the ac frequency ω (Fig.3.2), and no phase shift and gain at other frequencies. For K_p, it is tuned in the same way as for a PI controller, and it basically determines the dynamics of the system in terms of bandwidth, phase and gain margin. To avoid instability associated with an infinite gain, (3.6) can be used instead of (3.5) to give a non-ideal PR controller and, as illustrated in Fig. 3.3, its gain is now finite, but still relatively

high for enforcing small steady-state error. Another feature of (3.6) is that, unlike (3.5), its bandwidth can be widened by setting ω_c appropriately, which can be helpful for reducing sensitivity towards slight frequency variation in a typical utility grid, K_i can be tuned for shifting the magnitude response vertically, but has no significant effect on bandwidth.

Besides single frequency compensation, selective harmonic compensation can also be achieved by cascading several resonant blocks tuned to resonate at the desired low-order harmonic frequencies to be compensated for. The equations (3.5) and (3.6) can be rewritten for employing PR controller as selective harmonic elimination which is given in equations (3.7) and (3.8) respectively.

$$G_h(s) = \sum_{h=3,5,7\ldots} \frac{2K_{ih}s}{s^2+\omega_h^2} \tag{3.7}$$

$$G_h(s) = \sum_{h=3,5,7\ldots} \frac{2K_{ih}\omega_c s}{s^2+2\omega_c s+\omega_h^2} \tag{3.8}$$

Where h is the harmonic order to be compensated for and K_{ih} represents the individual resonant gain, which is to be tuned relatively high (but within stability limit) for minimising the steady-state error. An interesting feature of the PR controller as harmonic eliminator is that it does not affect the dynamics of the fundamental PR controller, as it compensates only for frequencies that are very close to the selected resonant frequencies.

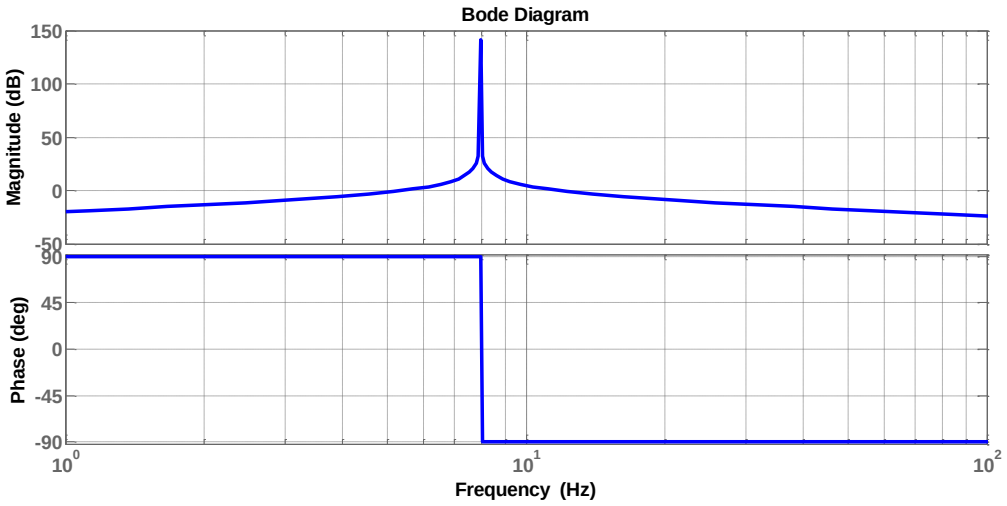

Fig. 3.2 Bode plots of ideal PR controller with K_i=20, ω=314 rad/sec

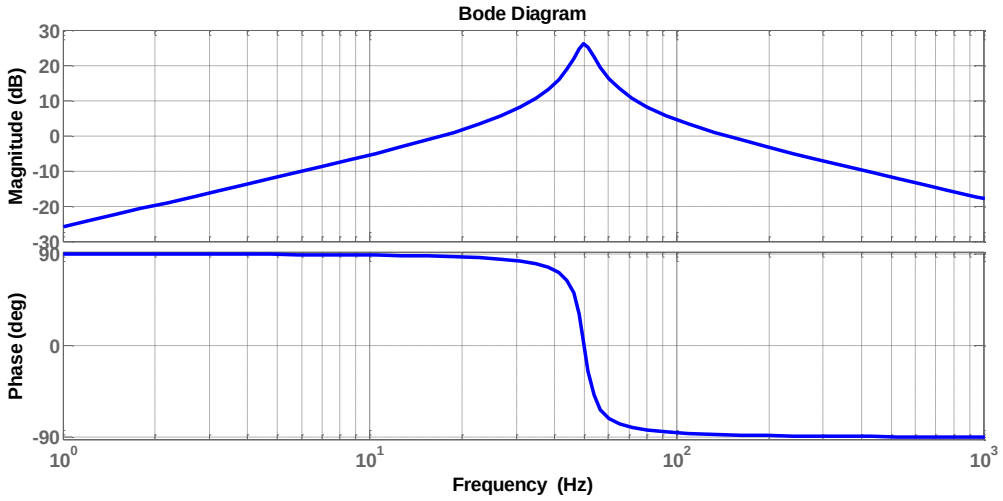

Fig. 3.3 Bode plots of non-ideal PR controller

with K_i=20, ω=314 rad/sec, ω_c= 20 rad/sec

Using a smaller ω_c will make the filter more sensitive to frequency variations, lead to a slower transient response.

3.1.1.A Current Control Scheme

An ACC is having advantage over peak current controller of adding a high gain in forward control path and hence reduces the steady state error [7]. Here the inductor current has been averaged over a switching period. And digital implementation of the current controller introduces a sampling delay. This delay yields 180° phase lag at the half of switching frequency. So digital delay of one switching period is introduced in the current loop whose transfer function is given by Eq (3.9) based on Padde's expansion.

$$RD(s) = \frac{1-\frac{sT_s}{2}+\frac{(sT_s)^2}{12}}{1+\frac{sT_s}{2}+\frac{(sT_s)^2}{12}} \tag{3.9}$$

As bipolar PWM [5] technique has been used to generate switching pulses for the inverter a gain F_m is included in the current loop. The gain F_m is given by equation (3.10).

$$F_m = \frac{1}{V_{pp\_Triangular}} \tag{3.10}$$

Here F_m is taken as 1. The control loop of ACC is shown in Fig 3.4.

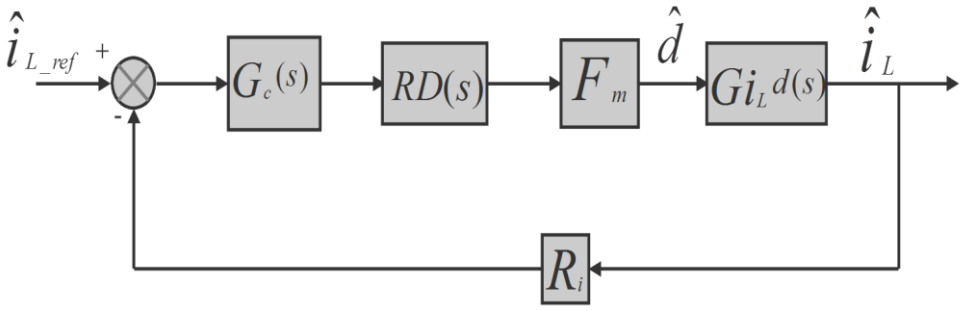

Fig.3.4 Control loop for ACC strategy

The reference value of inductor current is generated from the output of voltage control loop discussed in the next section. A current sensor is being used to sense inductor current and its gain R_i is considered for controller design. In this research work its value is taken as 0.2. The transfer function for the design of current loop is the ratio between duty cycle to output current ($Gi_Ld(s)$) and is given by equation (3.11) which has been deduced from small signal model of inverter (Fig.2.4) by keeping $\widehat{v_{dc}} = 0$.

$$Gi_Ld(s) = \frac{2V_{dc}}{Z+sL} \tag{3.11}$$

Where Z= load impedance is given by equation (3.12)

$$Z = \frac{(R_cC.s+1).R}{C.s(R_c+R)+1} \tag{3.12}$$

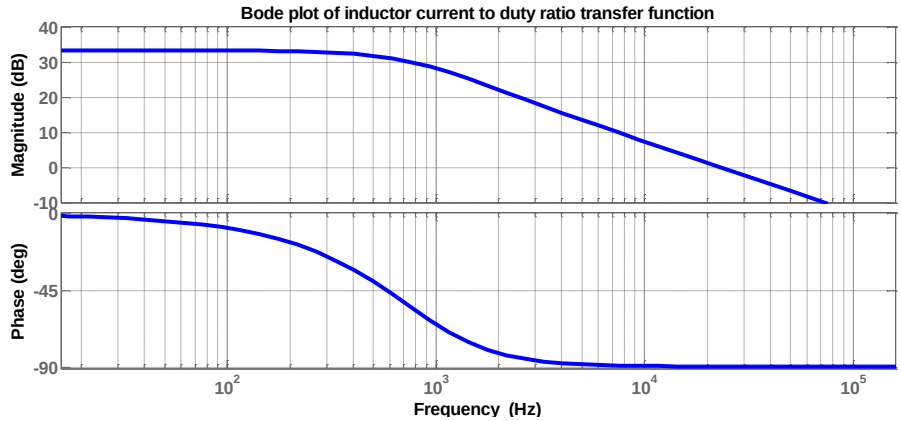

Fig.3.5 Bode plot of $Gi_Ld(s)$

As shown in the bode plot of $Gi_Ld(s)$ phase cross over frequency is 10kHz which gives flatter response to inductor current which is due to implementation of ACC.

For the current loop a proportional and resonant controller has been chosen. An ideal resonant controller adds an infinity gain to the control loop so as to reduce the steady state error. But, practically it's not feasible. In this work it adds a finite but high gain value to the current loop which can be clearly observed from bode plot of current loop as depicted in Fig.3.6.

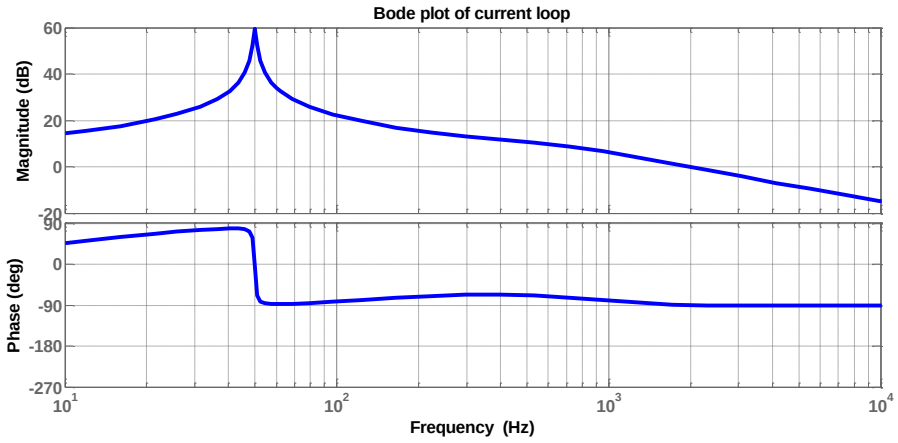

Fig.3.6 Bode plot of current loop

The transfer function of chosen proportional and resonant control is given by equation (3.13)

$$G_c(s) = K_p + \frac{K_1 B_1 s}{s^2 + B_1 s + {\omega_1}^2} \tag{3.13}$$

For this application gain K_1=100, bandwidth B_1=2.π rad and the resonant angular frequency ω_1=2.π.50 rad/sec. It can be observed from Fig.3.3 that at resonant frequency (i.e 50Hz) a high gain is being added to loop and there is a phase drop simultaneously. The current loop is having phase margin of 90° and gain cross over frequency is 1.9 kHz. The value of K_p has been chosen as 0.3859.

3.1.1.B Voltage Control Scheme

The voltage controller is meant for controlling the output voltage of the inverter and it generates reference current for the current controller (ACC). In this research work two types of controllers for voltage control have been implemented and compared. The bode plot of voltage control loop is given in Fig.3.7.

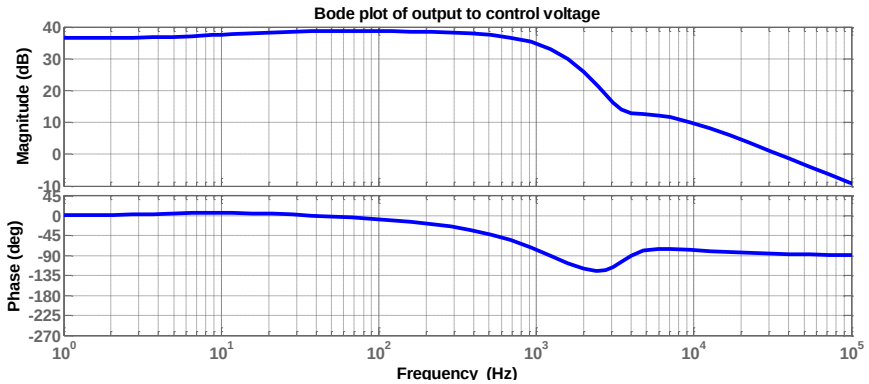

Fig.3.7 Bode plot of $G_{v_0-v_c}$

The control to output voltage transfer function is considered for designing a controller given by equation (3.14).

$$G_{v_0-v_c} = \frac{\hat{v}_0}{\hat{v_c}} \tag{3.14}$$

3.1.1.B.1 PI Voltage Controller

The PI controller produces a system response with minimized steady state error in the output. The integral action reduces the error produced by the proportional action. The control scheme of the inverter including voltage control is given in Fig.3.8. Like current sensor, a voltage sensor of gain β is used to sense the output voltage of inverter. In this work the gain of the voltage sensor is assumed as 0.006.

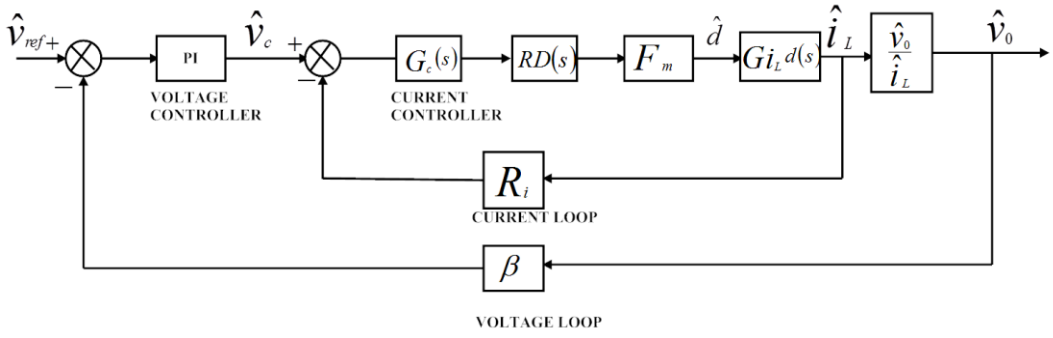

Fig.3.8. ACC with PI controller

The value of the gain of the PI controller has been derived from the step response of the plant transfer function and is given by equation (3.15) and the bode plot of voltage loop with PI controller is given in the Fig.3.9.

$$PI(s) = 0.20448.\frac{s+4270}{s} \tag{3.15}$$

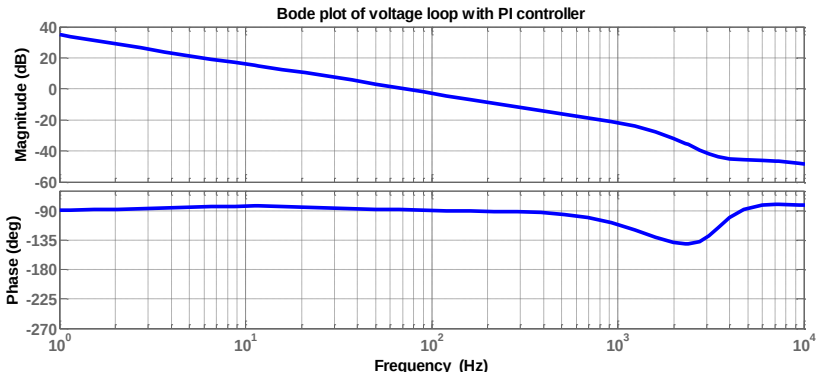

Fig.3.9 Bode plot of voltage loop with PI controller

The transfer function of the voltage loop with PI controller is given by equation (3.16) which has been deduced from Fig.3.8. From Fig 3.8 it was found that the gain cross over frequency of the voltage loop is 70 Hz and the phase margin is 91º.

$$T_v(s) = G_{v_0 - v_c}(s).\beta.PI(s) \tag{3.16}$$

3.1.1.B.2 Resonant Voltage Controller

In this work a proportional and resonant controller was implemented along with ACC so as to reduce THD in grid voltage. This controller is meant for improving the reference tracking and the attenuation of multiple fundamental spectral components. The transfer function of the proportional and resonant controller is given by equation (3.17).

$$G_{v\_res}(s) = K_p + \sum_{h=1}^{9} \frac{K_h.B_h.s}{s^2 + B_h.s + \omega_h^2} \tag{3.17}$$

Where h= odd no.

K_h=gain of h^{th} harmonic

B_h= bandwidth of h^{th} harmonic

K_p= gain of the proportional controller and in this case 0.26.

The control structure is illustrated in the Fig.3.10, where a proportional controller has been implemented with resonant controller. In this work resonator for harmonics up to 9^{th} have been considered which helps in reducing those dominant lower order harmonics.

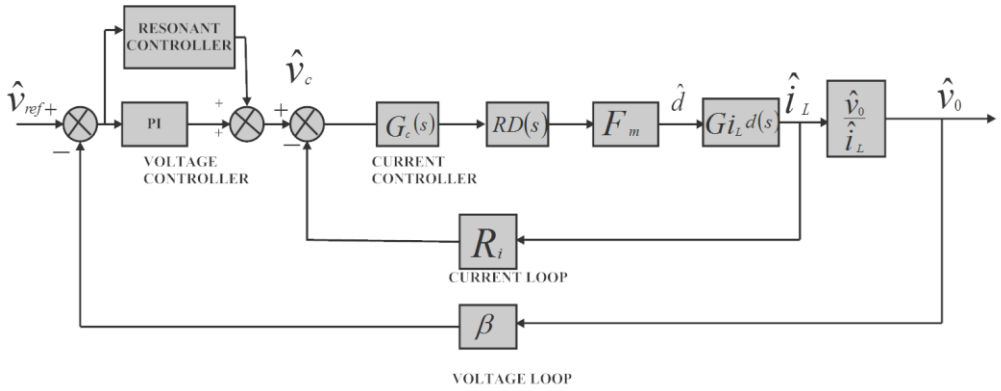

Fig.3.10 ACC with P+Resonant controller

The values of the gains of odd harmonics and their bandwidths have been given in the Table 3.1 [14].

Table 3.1

Resonant Controller Parameters

Harmonic order	Gains	Bandwidth
1	28	π
3	12	3π
5	8	5π
7	6	7π
9	4	9π

From the bode plot of voltage loop with proportion and resonant controller as shown in Fig.3.11 it can be observed that the phase is zero at the harmonic frequencies, this means that the controller has a resistive behavior. The decreasing value at high frequencies allows a reduction in the harmonic voltage and hence reduction in voltage THD.

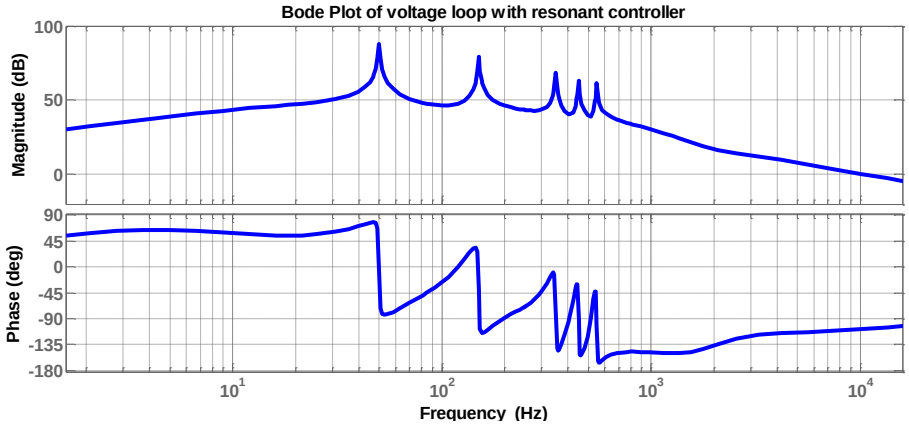

Fig.3.11 Bode plot of voltage loop with P+ Resonant controller

$$T_v(s) = G_{v\_res}.G_{v_0-v_c}.\beta \tag{3.18}$$

The bode plot was obtained from equation (3.18) and Fig.3.10. From the bode plot, the gain cross over frequency is found to be 10 kHz and the phase margin is 80º. The system parameters of the concerned 1-Φ inverter are given in Table.3.2.

Table 3.2

System Parameters (1-Φ)

SL. No.	Parameters	Values
1.	Dc link voltage (V_{dc})	400 V
2.	Inverter Output Voltage(V_0)	230 V_{rms}
3.	Inverter Output Frequency(f)	50 Hz
4.	Filter Inductance(L)	5.46 mH
5.	Filter Capacitance(C)	4.7 µF
6.	Damping Resistance(R_c)	5 Ω
7.	Inverter Switching Frequency(f_s)	16 kHz
8.	Load Resistance(R_{Load})	17.16 Ω

CHAPTER 4

4.1 Modelling of 3-Φ VSI

Three phase VSIs are used to interface between dc and ac systems in distributed power generation system. Different control techniques have been applied to the three phase grid connected VSI for the control of active and reactive power along with constant dc link voltage. However, designing a controller with help of a small signal model is a well-known practice in dc-dc converter. Transfer functions of the control variables need to be identified for designing a control system. The transfer functions are deduced using averaged switched modeling technique. In modern days power electronics converters are widely employed in all the applications. As the switches are involved in these applications, non-linearity occurs in the system. So the power stage must be linearized in order to design a linear feed-back control. In this work a three phase grid connected VSI with LC filter has been considered for modeling. As it is quite difficult to design a controller in case of three phase ac system, so first three phase ac system (abc) is transformed into synchronous rotating reference frame (dq) and the transformation is known as Park's transformation [17]. The resulting model from the corresponding transformation is known as large signal model which involves dc quantities due to the transformation to the rotating reference frame.

The modeling of inverter involves two stages namely power stages modeling which is said to be large signal modeling and small signal modeling.

4.1.1. Power Stage Model

In power stage of model the power circuit, second order LC filter, grid and corresponding parameters are transformed in to synchronous rotating reference frame.

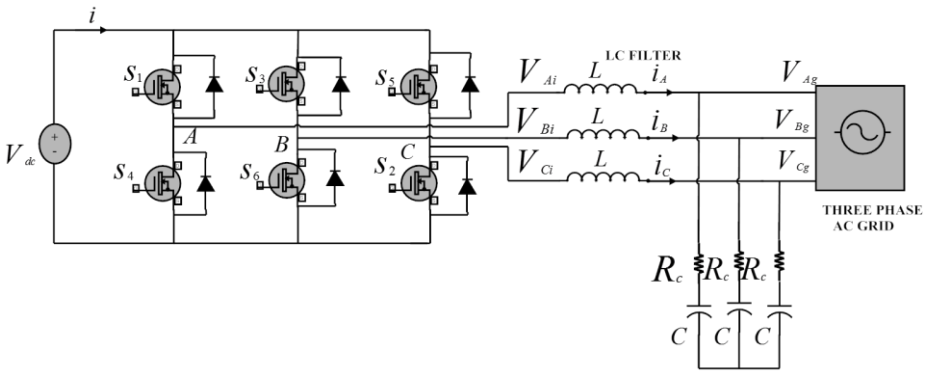

Fig.4.1 Schematic diagram of three phase grid connected VSI with LC filter

In Fig.4.1 three phase VSI is connected to the grid through a LC filter. V_{Ai},V_{Bi} ,V_{Ci} are the voltages at the inverter output and V_{Ag} ,V_{Bg}, V_{Cg} are the voltages at the grid end. By applying voltage balance equation

$$\Rightarrow \begin{bmatrix} V_{Ai} \\ V_{Bi} \\ V_{Ci} \end{bmatrix} = L\frac{d}{dt}\begin{bmatrix} i_a \\ i_b \\ i_c \end{bmatrix} + \begin{bmatrix} V_{Ag} \\ V_{Bg} \\ V_{Cg} \end{bmatrix} \tag{4.1}$$

where L= inductance with negligible resistance.

By transforming the equation (4.1) into synchronous reference frame as given in Appendix A the following equation (4.2) is obtained.

$$\Rightarrow \begin{bmatrix} V_{di} \\ V_{qi} \end{bmatrix} = L\frac{d}{dt}\begin{bmatrix} i_d \\ i_q \end{bmatrix} + \begin{bmatrix} V_{dg} \\ V_{qg} \end{bmatrix} + \omega L\begin{bmatrix} -i_q \\ i_d \end{bmatrix} \tag{4.2}$$

As the inverter output voltage is a function of dc link voltage, the inverter dq-voltages are expressed as follows

$$\begin{bmatrix} V_{di} \\ V_{qi} \end{bmatrix} = \begin{bmatrix} d_d \\ d_q \end{bmatrix} V_{dc} \tag{4.3}$$

$$\&\quad i = [d_d \quad d_q].\begin{bmatrix} i_d \\ i_q \end{bmatrix} \tag{4.4}$$

Where V_{dc} is dc link voltage applied to the inverter and d_d and d_q are the duty cycles corresponding to the d- and q-axes respectively. By substituting value of equation (4.3) in equation (4.2), equations (4.5) and (4.6) are obtained

$$d_d.V_{dc} = L\frac{di_d}{dt} - \omega L i_q + V_{dg} \tag{4.5}$$

$$d_q.V_{dc} = L\frac{di_q}{dt} + \omega L i_d + V_{qg} \tag{4.6}$$

The compensating terms appearing in the equations (4.5) and (4.6) are due to the mutual inductance effect. From the above equations power stage model can be deduced and the corresponding model is depicted in Fig.4.2.

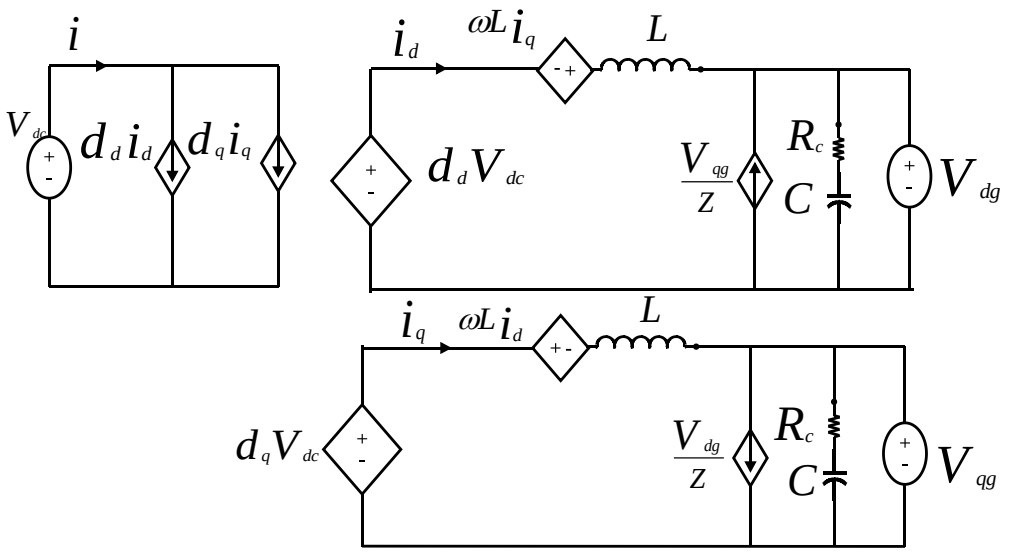

Fig.4.2 Power stage model of three phase grid connected VSI

In Fig.4.2 R_c is the damping resistor used to damp out the oscillations occurring due to the resonance resulted from LC filter. The values of L, C (filter capacitance) and damping resistor R_c have been referred from [14]. Power stage model is helpful in getting a dc operating point so as to design a controller for it. Z is the output impedance given by equation (4.7)

$$Z = \sqrt{\left(R_c{}^2 + \left(\frac{1}{\omega C}\right)^2\right)} \tag{4.7}$$

4.1.2 Small Signal Model

The small signal model is then derived from the power stage model similar to 1-Φ inverter modeling by giving a perturbation and then linearizing around an operating point for stable and fast response.

An operating point is defined as follows;

Dc supply voltage= V_{dc}

d-axis duty cycle= D_d

q-axis duty cycle= D_q

d-axis current = I_d

q-axis current = I_q

d-axis grid voltage= V_{dg}

q-axis grid voltage= V_{qg}

For deriving small signal model a perturbation is given around the operating point which is given as follows

$V_{dc} = V_{dc} + \widehat{v_{dc}}$

$D_d = D_d + \widehat{d_d}$

$D_q = D_q + \widehat{d_q}$

$I_d = I_d + \widehat{\imath_d}$

$I_q = I_q + \widehat{\imath_q}$

$V_{dg} = V_{dg} + \widehat{v_{dg}}$

$V_{qg} = V_{qg} + \widehat{v_{qg}}$

In the above new operating point, parameters with 'ʌ' are the small perturbed variables. By adapting these perturbations in equations (4.3), (4.4), (4.5) & (4.6) and neglecting the steady and non-linear terms, equations (4.8), (4.9) and (4.10) can be obtained

$$L\frac{d\widehat{\imath_d}}{dt} = \widehat{v_{dg}} - D_D\widehat{v_{dg}} - \widehat{d_d}V_{dc} - \omega L i_q \quad (4.8)$$

$$C\frac{d\widehat{v_{dg}}}{dt} = \widehat{\imath_d} + \frac{\widehat{v_{qg}}}{Z} \quad (4.9)$$

$$\hat{\imath} = D_d\widehat{\imath_d} + D_q\widehat{\imath_q} + \widehat{d_d}I_d + \widehat{d_q}I_q \quad (4.10)$$

Based on the above three equations small signal model of grid connected inverter has been derived and shown in Fig.4.3.

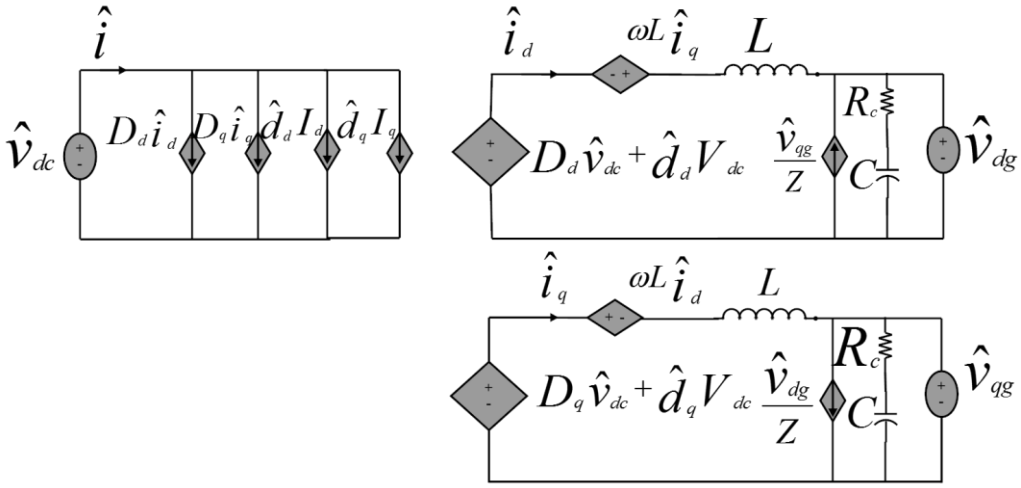

Fig.4.3 Small signal model of three phase grid connected VSI

In the modeled 3-Φ VSI small signal current $\hat{\imath}$ is drawn by VSI from the source $\widehat{v_{dc}}$which is a function of control signal and its variations and hence it is shown as a dependent source. Due to transformation to synchronous rotating frame (dq) two dependent circuits have been resulted. Both circuits are still cross coupled with each other due to the effect of mutual induction. For the simplicity it is assumed that grid voltage is oriented along d-axis and hence $\widehat{v_{qg}}$ is considered to be zero.

CHAPTER 5

5.1 Transfer Functions and Bode Plots

The small signal model illustrated in Fig.4.3 is then used to extract open loop transfer functions. The transfer functions of interest are 1. Control function to the filter inductor currents 2.Control function to the grid voltages.

For simplification in deriving transfer functions the grid voltage is oriented along d-axis. So V_{dg} is of constant amplitude as grid voltage is having constant amplitude and V_{qg} =0. From Fig.4.3 concerned transfer functions are derived in frequency domain and are explained as follows

5.1.1 Control to d-axis Current Transfer Function:

This transfer function is obtained from the derived small signal model by assuming $\widehat{v_{dc}} = 0$.

$$\frac{\widehat{i_d}}{\widehat{d_d}} = \frac{V_{dc}}{sL+Z} \tag{5.1}$$

5.1.2 Control to Grid Voltage Transfer Function:

Similarly grid voltage transfer function is developed from the small signal model.

$$\frac{\widehat{v_{dg}}}{\widehat{d_d}} = \frac{V_{dc}Z}{sL+Z} \tag{5.2}$$

Bode plots of control to grid voltage transfer function and control to grid current transfer function is given in Fig.5.1 and Fig.5.2 respectively.

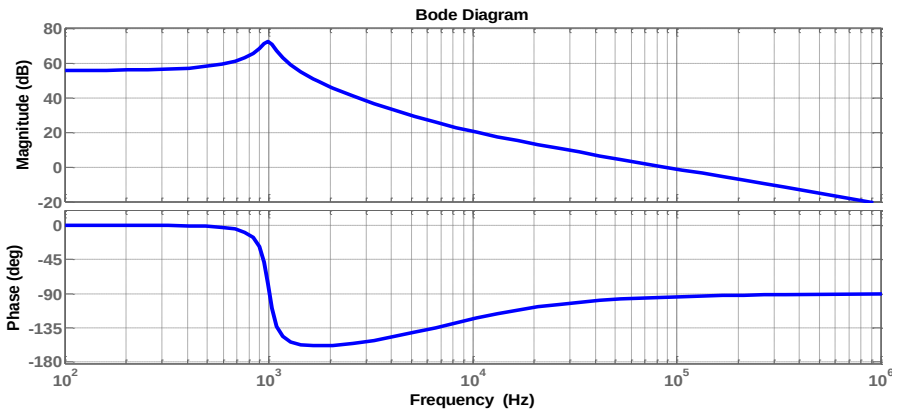

Fig.5.1 Control to grid voltage transfer function bode plot

As LC filter is incorporated between the inverter and grid, it is prone to occurrence of resonance [18]. The resonant frequency is given as follows

$$\omega_0 = \frac{1}{\sqrt{LC}} \tag{5.3}$$

In this work resonant frequency f_0 is 993Hz by considering the values of L and C from given in Table.5.1. In Fig.5.1 resonance can be observed i.e at the frequency of 993 Hz there is a phase drop of 45° and at the same time there is a peak in the magnitude plot. However, a suitable damping resistor R_c is used for damping out the oscillations at resonant peak.

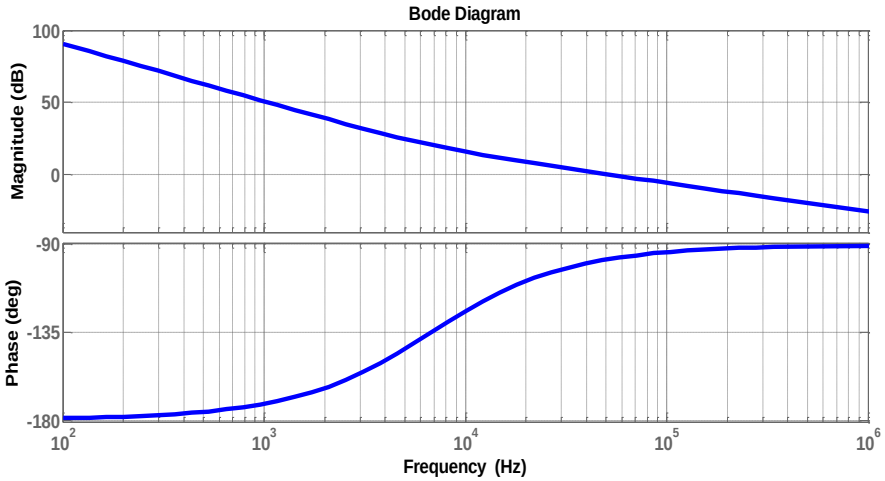

Fig.5.2 Control to grid voltage transfer function bode plot

From Fig.5.2 the phase margin is 80 degree which confirms the stability of the system. The phase cross over frequency is 100Hz and the gain cross over frequency is 10.4 kHz.

Table.5.1

System Parameters (3-Φ)

SL. No.	Parameters	Values
1.	Dc link voltage (V_{dc})	600 Volt
2.	Inverter output frequency (f)	50Hz
3.	Filter inductance (L)	5.46 mH
4.	Filter capacitance(C)	4.7 µF
5.	Damping resistance(R_c)	5 Ω
6.	Dc link capacitance	1800 µF

5.2 Control Strategy for 3-Φ Inverter

The main purpose of control strategy of 3-Φ grid connected inverter is to control the active and reactive power flow independently. Control variable i_d is used for active power control and i_q is used for reactive power control. A control strategy is developed by using equation (4.8). The control algorithm is depicted in Fig.5.3.

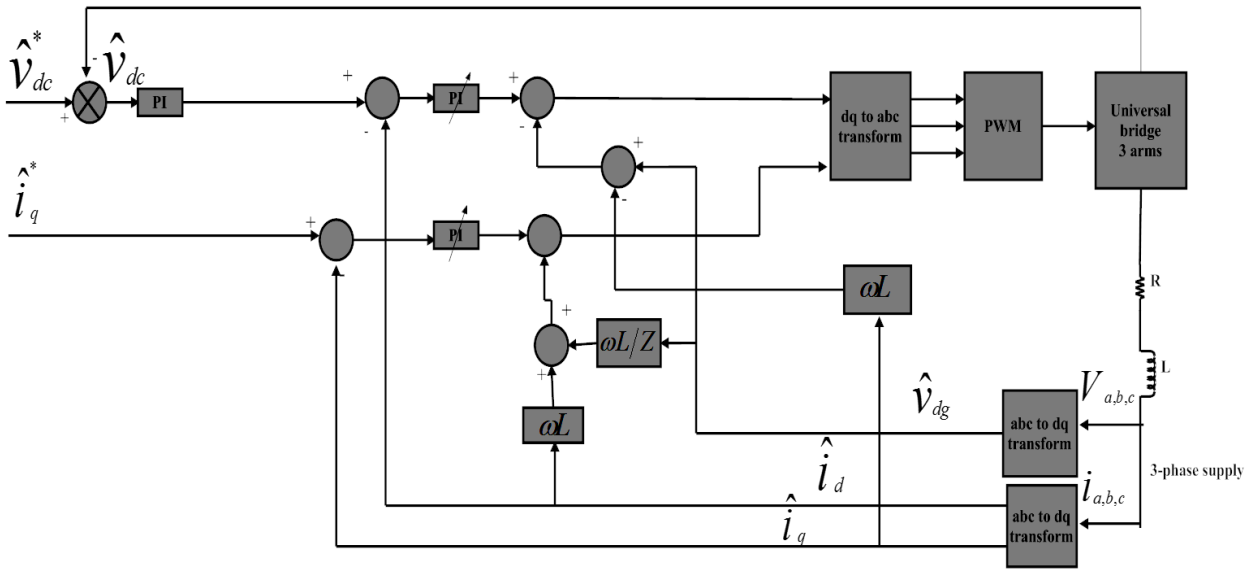

Fig.5.3 Control structure of 3-Φ grid connected VSI

For the transient study and to design a control strategy for controlling the active and reactive power independently transformation of three phase system (abc) to synchronous rotating reference frame is preferred.

Let's consider the system after the application of Park's transformation [18] and

V_d = d-axis voltage

V_q= q-axis voltage

I_d= d-axis current

I_q= q-axis current

P= active power

Q= reactive power

S= apparent power

As d-axis and q-axis are of 90 deg phase difference with each other the voltage and current can be expressed as depicted in equation (5.4) and (5.5)

$V_{dq}= V_d+jV_q$ (5.4)

$I_{dq}= I_d+jI_q$ (5.5)

It is well known the apparent power $S= I^*_{dq}V_{dq}$ (5.6)

By substituting values of V_{dq} and I_{dq} from equations (5.4) and (5.5) in equation (5.6), equation (5.7) is derived

$S= (V_dI_d+V_qI_q)+j(V_qI_d-V_dI_q)$ (5.7)

According to PCC voltage orientation frame V_d is assumed as the maximum value of grid voltage and V_q=0. By substituting this condition in equation (5.7) active power and reactive power are derived as follows

$P= V_dI_d$ (5.8)

& $Q= -V_dI_q$ (5.9)

The negative sign in the reactive power signifies that it can flow in either direction i.e from inverter to grid and vice versa. For the control algorithm the d-axis reference current is generated from equation (5.8) and also it can be generated from the dc-link voltage error and the q-axis reference current is generated from equation (5.9). So in other words control of d-axis current (I_d) is done for active power control and that of q-axis (I_q) for reactive power control.

CHAPTER 6

6.1 Results and Discussions

6.1.1 1-Φ Inverter

The simulation was carried out based on system parameters given in Table.3.2 in MATLAB/Simulink environment. In this part output voltage and current waveforms of inverter have been shown. For nonlinear load a full wave rectifier with capacitive filter of 370μF and a resistance of 50Ω have been used. All the simulations were performed in isolated mode. Then THD of output voltage was calculated by FFT analysis and the obtained results are compared.

6.1.1.A With PI Voltage Controller

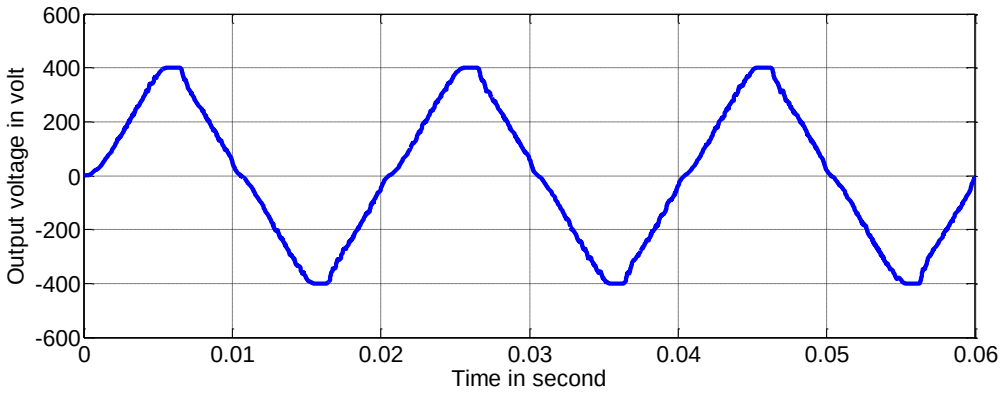

Fig.6.1 Output voltage (V_0) waveform of inverter (linear load)

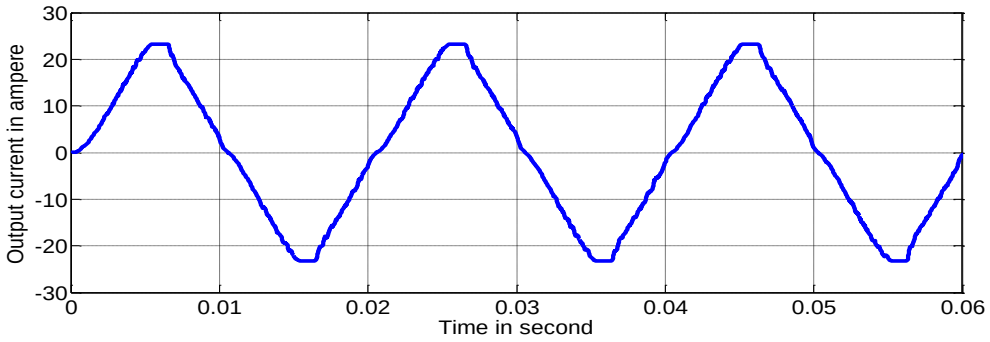

Fig.6.2 Output voltage (i_0) waveform of inverter (linear load)

Here for linear load a resistance of 17.16 ohm is connected across inverter output. As the input dc supply is of 400 volt, an AC voltage of peak value 400volt is obtained across output. The corresponding load limit is 23.31 ampere is opted as load current. Though output

waveforms are approaching sinusoidal, yet output voltage contains some higher order harmonics. Corresponding harmonic spectrum of output voltage is shown in Fig 6.3 and it found that the THD of V_0 is 2.81%.

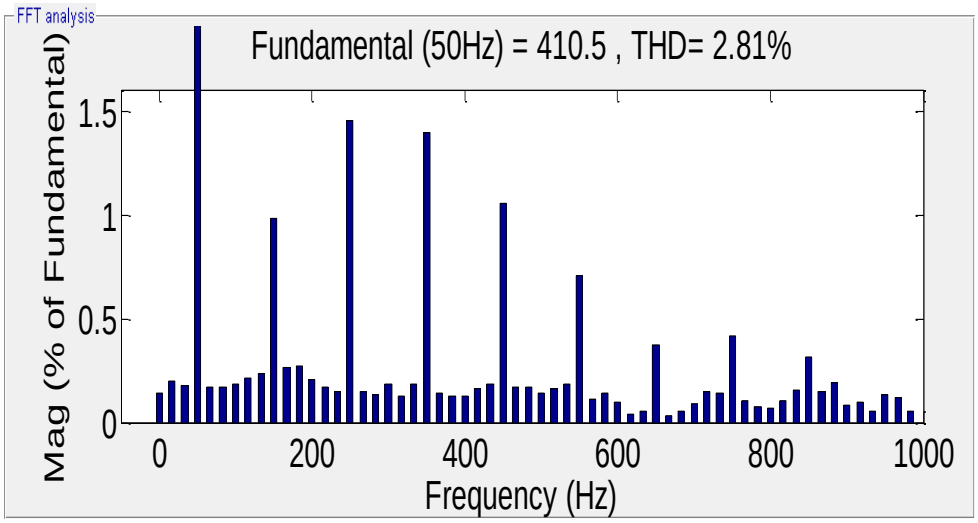

Fig.6.3 THD of output voltage for linear load

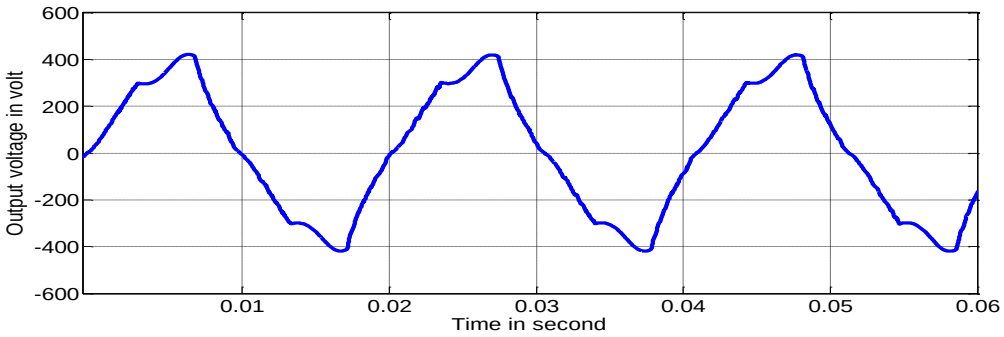

Fig. 6.4 Output voltage (V_0) waveform of inverter (non-linear load)

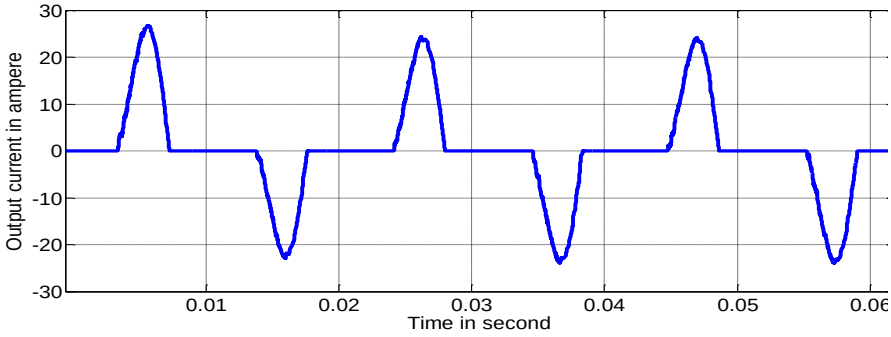

Fig. 6.5 Output voltage (i_0) waveform of inverter (non-linear load)

For a non-linear load a rectifier load is considered. As the rectifier uses switching devices, hence generates harmonics and then injects to source. Hence output voltage as well as output

current is containing harmonics. As a result they are not sinusoidal which is expected to be so. When output voltage was analyzed through FFT the THD was found to be 15.08% given in Fig.6.6.

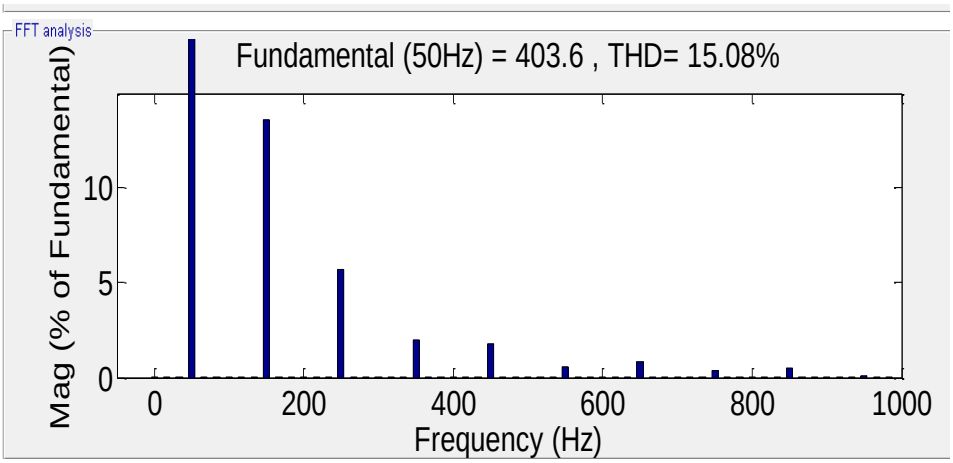

Fig.6.6 THD of output voltage for non-linear load

6.1.1.B With P+Resonant Voltage Controller

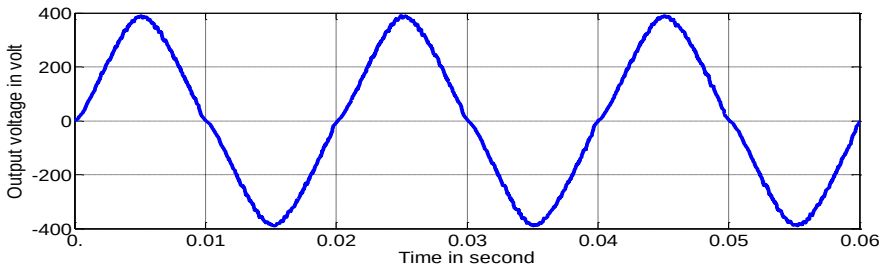

Fig.6.7 Output voltage (V_0) waveform of inverter (linear load)

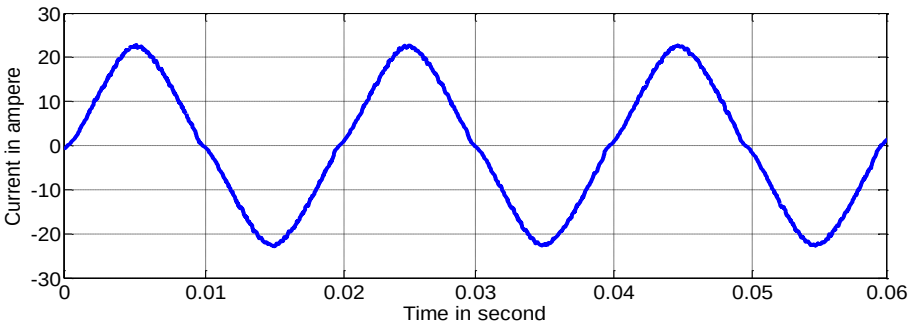

Fig.6.8 Output voltage (i_0) waveform of inverter (linear load)

As resonant controller is based on principle of resonance, it outperforms the PI controller. In Fig 6.7 & 6.8 output voltage and current are nearly sinusoidal. Its FFT analysis gives the THD of 0.69% given in Fig.6.9.

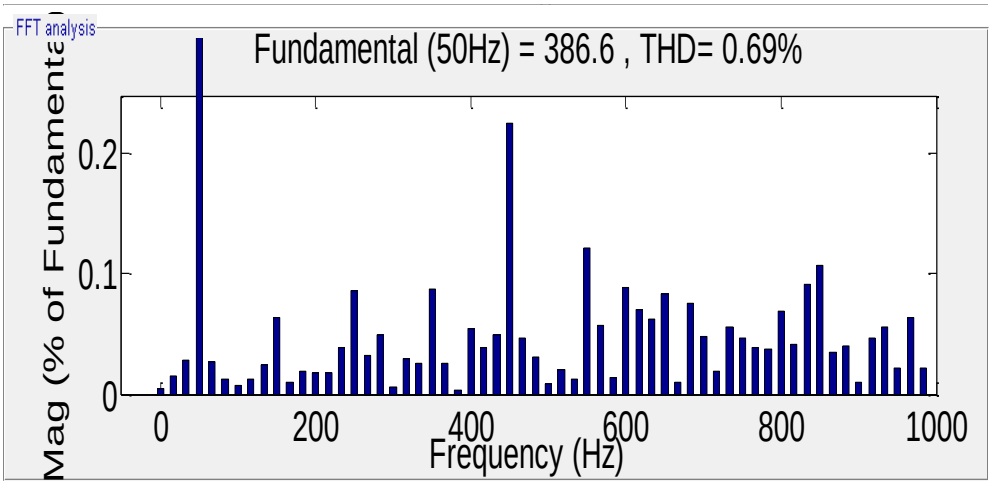

Fig.6.9 THD of output voltage for linear load

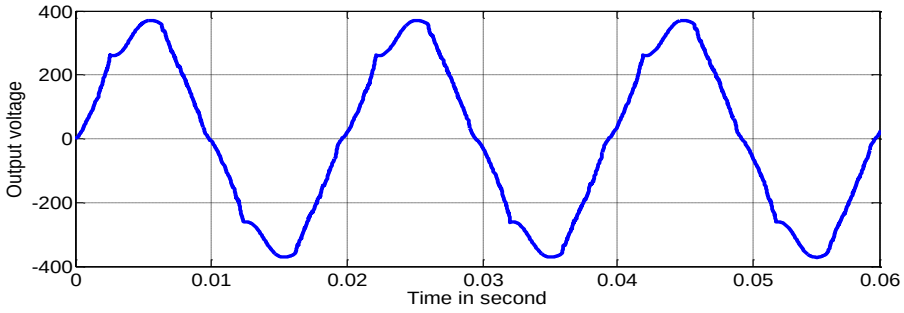

Fig.6.10 Output voltage (V_0) waveform of inverter (non-linear load)

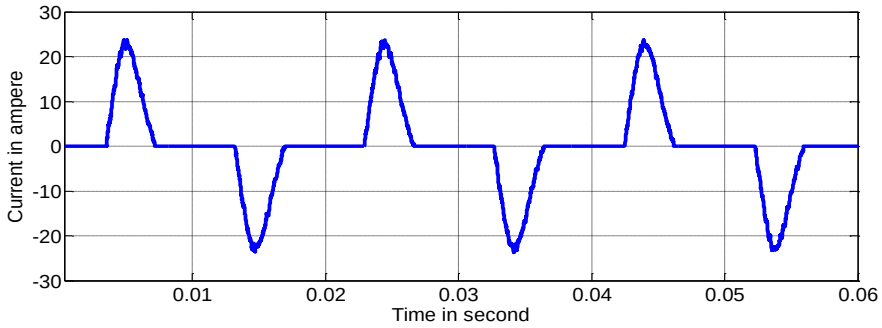

Fig.6.11 Output voltage (V_0) waveform of inverter (non-linear load)

When this resonant controller along with ACC is implemented in case of nonlinear load it shows better performance than PI controller. FFT analysis of output voltage gives THD of 7.53% given in Fig.6.12.

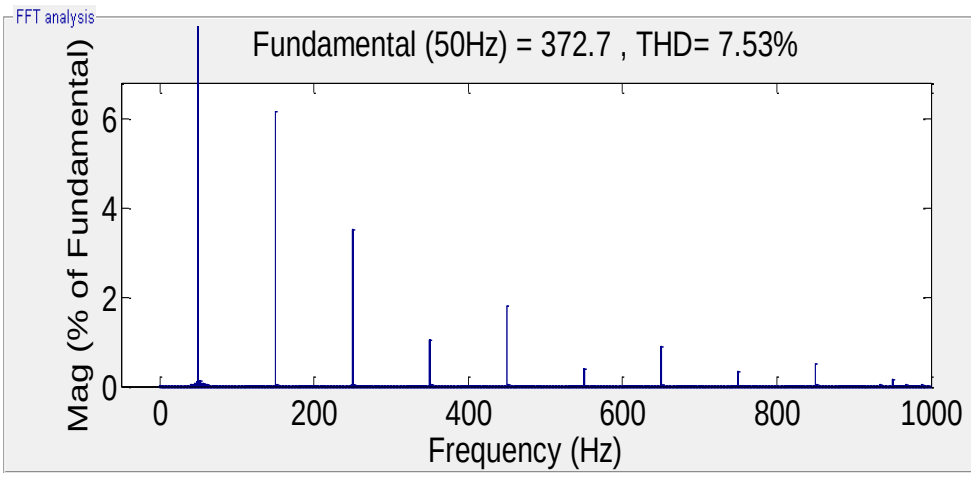

Fig.6.12 THD of output voltage for non-linear load

6.1.1.C. . Comparison of THD%

Sl.No.	Controller	Linear load	Nonlinear load
1.	PI	2.81%	15.03%
2.	P+Resonant	0.69%	7.53%

6.1.2. 3-Φ Inverter

Based on the deduced transfer functions the step responses of the voltage and current controller of the three phase grid connected inverter are plotted in the MATLAB/Simulink environment.

1. Step response of dc link voltage controller

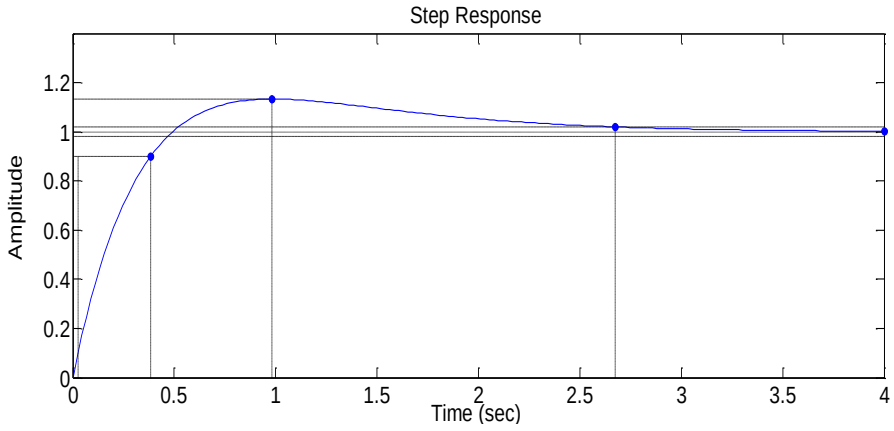

Fig.6.13 Step response of dc link voltage controller

In the Fig.6.13 step response of the dc-link voltage controller is shown. As the dc-link voltage controller is a slower one its rise time is set at 0.059 second. Its settling time is 2.675 second and having a peak overshoot of 13.3%.

2. Step response of inner current controller

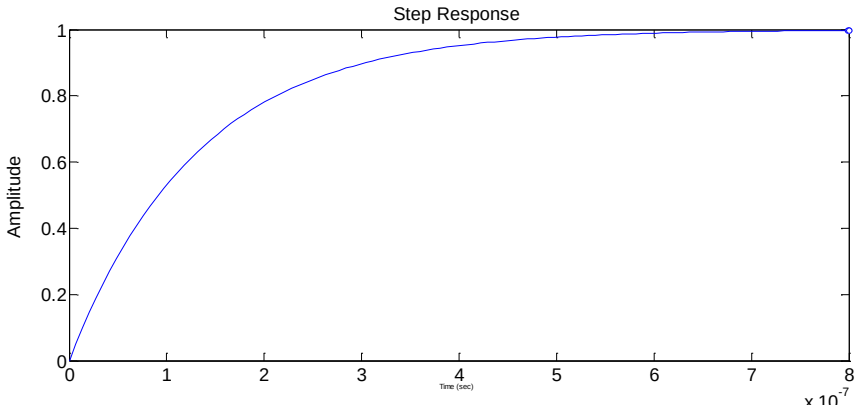

Fig.6.14.Step response of current controller

In Fig.6.14 step response of the current compensator is shown. As the current controller is the faster one it's rise time is set to lesser than that of outer dc-link voltage controller. A control strategy is based on the goal of minimizing absolute error between the desired and the actual d-axis and q-axis currents through an adaptive tuning process. It is crucial to identify that fast current loop controller is necessary to assure highest power quality.

CHAPTER 7

7.1 Conclusion and Future scope of work

In this thesis a small signal model of a 1-Φ inverter is derived and an Average current controller was developed, further bode plots were plotted based on the transfer functions of the derived model. A comparison has been made for the THD% of output voltage with two different type of voltage controllers i.e PI and Resonant controller. From the obtained results it is concluded that P+Resonant controller gives less THD% in output voltage in case of both linear as well as non-linear load as compared to PI voltage controller. In addition to that observation feasibility of the study with theoretical results the modeling was extended to three phase grid connected inverter with LC filter. From the derived small signal model transfer functions were derived and bode plots were plotted to study stability. The effect of resonance was observed from the bode plot of control to output voltage transfer function. A control strategy was developed based on the model and its step responses were plotted. Based on the small signal model of three phase grid connected inverter controller can be developed in order to regulate active and reactive power during grid abnormalities.

References

[1] Andreas Poullikkas, “Implementation of distributed generation technologies in isolated power systems,” Renewable and Sustainable Energy Reviews, Volume 11, Issue 1, Pages 30-56, January 2007.

[2] N.W.A. Lidula and A.D. Rajapakse,“Micro-grids research: A review of experimental micro-grids and test systems, Renewable and Sustainable Energy Reviews, Volume 15, Issue 1, Pages 186-202, January 2011.

[3] Balduino Cezar Rabelo, Joao Lucas Da Silva, Rodrigo Gaiba de Oliveria and Selenio Rocha Silva, “Reactive Power Control Design in Doubly Fed Induction Generators for wind Turbines. *IEEE Transactions on Industrial Electronics* vol.56 no.10, oct,2009.

[4] “Indian Wind Energy and Economy,” Indian wind power.com. Retrieved 2009-09-17.

[5] N Mohan, TM Underland, WP Robbins. “Power electronics: converters, applications, and design. 3rd ed. John Wiley & sons: 2003.

[6] RW Erickson. “Fundamental of Power Electronics. Norwell, MA:Kluwer; 1997”.

[7] Jian Sun and Bass Richard M., "Modeling and practical design issues for average current control," Applied Power Electronics Conference and Exposition, 1999. APEC '99. Fourteenth Annual , vol.2, no., pp.980-986 vol.2, 14-18 Mar 1999.

[8] Jinhaeng Jang, Seokjae Choi, Byungcho Choi and Sungsoo Hong, "Average current mode control to improve current distributions in multi-module resonant dc-to-dc converters," Power Electronics and ECCE Asia (ICPE & ECCE), 2011 IEEE 8th International Conference, vol., no., pp.2312-2319, May 30 2011-June 3 2011.

[9] Thibault R., Al-Haddad K. and Dessaint L.A., "A new control algorithm for 3-phase PWM voltage source converters connected to the grid," Electrical and Computer Engineering, 2005. Canadian Conference, vol., no., pp.1274-1277, 1-4 May 2005.

[10] Jaime Castelló Moreno, José M. Espí Huerta, Rafael García Gil and Sergio Alejandro González, “A Robust Predictive Current Control for Three-Phase Grid-Connected Inverters”. *IEEE Transactions on Industrial Electronics*, vol. 56, no. 6, June 2009.

[11] Juan C. Vasquez, Josep M. Guerrero, Alvaro Luna, Pedro Rodríguez and Remus Teodorescu, “Adaptive Droop Control Applied to Voltage-Source Inverters Operating in Grid-Connected and Islanded Modes”. *IEEE Transactions on Industrial Electronics*, vol. 56, no. 10, October2009.

[12] Shuhui Li, Timothy A. Haskew, Yang-Ki Hong and Ling Xu, "Direct-current vector control of three-phase grid-connected rectifier–inverter," Electric Power Systems Research, Volume 81, Issue 2, Pages 357-366, February 2011.

[13] Jiabing Hu, Lei Shang, Yikang He and Z. Q. Zhu, "Direct Active and Reactive Power Regulation of Grid-Connected DC/AC Converters Using Sliding Mode Control Approach". *IEEE Transactions on Power Electronics*, vol. 26, no. 1, January 2011.

[14] R. Ortega, E. Figueres, G. Garcerá, C.L. Trujillo and D. Velasco, "Control techniques for reduction of the total harmonic distortion in voltage applied to a single-phase inverter with nonlinear loads: Review," Renewable and Sustainable Energy Reviews, Volume 16, Issue 3, Pages 1754-1761, April 2012.

[15] Li-Chun Liao, Ming-Yu Lin and Chi-Hung Lin, "The large-signal SFG model for cascaded multilevel inverters with experimental verification," Power Electronics Conference (IPEC), 2010 International, vol., no., pp.2465-2468, 21-24 June 2010.

[16] Ning He, DehongXu, YeZhu, JunZhang, GuoqiaoShen, Yangfan Zhang, Jie Ma and Changjin Liu, "Weighted Average Current Control in a Three-Phase Grid Inverter With a LCL Filter". *IEEE Transactions on Power Electronics*, vol. 28, no. 6, June 2012

[17] Park, R.H., "Two-reaction theory of synchronous machines generalized method of analysis-part I," American Institute of Electrical Engineers, Transactions, vol.48, no.3, pp.716-727, July 1929.

[18] Ahmed K.H., Finney S.J. and Williams B.W., "Passive Filter Design for Three-Phase Inverter Interfacing in Distributed Generation," Compatibility in Power Electronics, 2007. CPE '07, vol. no., pp.1-9, May 29 2007-June 1 2007.

[19] Daniel E. Rivera, Manfred Morari, and Sigurd Skogestad, "Internal Model Control: PID Controller Design," Industrial & Engineering Chemistry Process Design and Development pp. 252-265, 1986.

[20] Teodorescu R., Blaabjerg F., Liserre M. and Loh, P.C., "Proportional-Resonant Controllers and Filters for Grid-Connected Voltage-Source Converters," Electric Power Applications, IEE Proceedings, vol.153, no.5, pp.750-762, September 2006.

[21] Newman M.J., Zmood D.N. and Holmes D.G.:, "Stationary Frame Harmonic Reference Generation for Active Power Filter Systems," *IEEE Trans. Ind. Appl.*, pp. 1591–1599,2002.

Appendix A (abc to dq transformation)

The transformation of three phases a-b-c is first done to two phase stationary reference frame i.e α-β reference frame and then to d-q reference frame which rotates at synchronous speed.

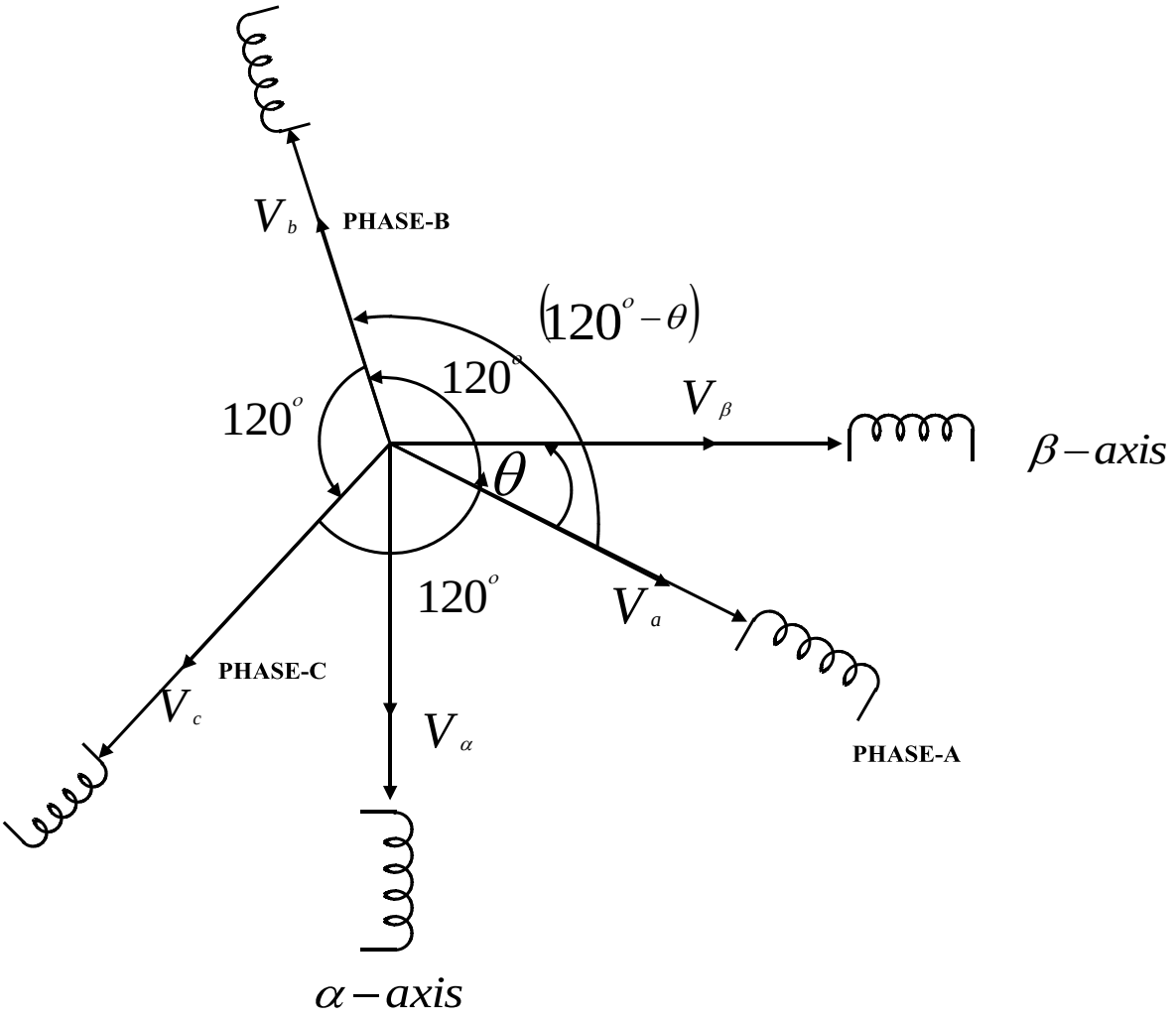

Fig.A1 Transformation of three phases to stationary α-β reference frame

$$\begin{bmatrix} V_\alpha \\ V_\beta \\ V_0 \end{bmatrix} = \frac{2}{3}\begin{bmatrix} \sin\theta & \sin(\theta-120^\circ) & \sin(\theta+120^\circ) \\ cos\theta & \cos(\theta-120^\circ) & \cos(\theta+120^\circ) \\ 0.5 & 0.5 & 0.5 \end{bmatrix} * \begin{bmatrix} V_a \\ V_b \\ V_c \end{bmatrix} \quad \text{(A.1)}$$

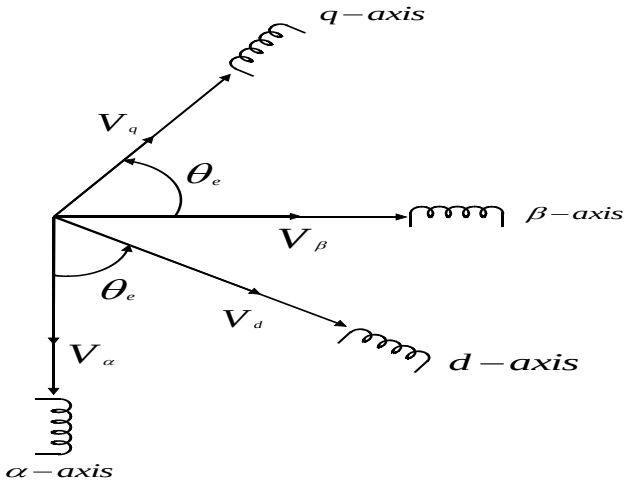

Fig.A2 Transformation of three phases to stationary α-β reference frame

$$\begin{bmatrix} V_\alpha \\ V_\beta \end{bmatrix} = \begin{bmatrix} cos\theta_e & -sin\theta_e \\ sin\theta_e & cos\theta_e \end{bmatrix} * \begin{bmatrix} V_d \\ V_q \end{bmatrix} \quad \text{(A.2)}$$

Publications

1. Tusar Kumar Dash and B. Chitti Babu, "A novel small signal modeling of three phase grid connected inverter system". In Proc.2nd IEEE student's conference on Engineering and systems, MNNIT Allahabad, Apr. 2013.

2. Tusar Kumar Dash and B. Chitti Babu, "Comparison of Control Techniques for Reduction of THD in 1-Φ Grid Interactive Inverter System". In Proc. IEEE sponsored 1st National Conference on Power Electronics and Systems, NIT Rourkela, pp. 315-319, Apr. 2013.